Martin Skaugset

Using Monte Carlo simulations to evaluate adaptive sampling strategies in synthetic and real ocean models

Master's thesis in Marine Technology
Supervisor: Martin Ludvigsen
Co-supervisor: Trygve O. Fossum

June 2021

◻ NTNU
Kunnskap for en bedre verden

Martin Skaugset

Using Monte Carlo simulations to evaluate adaptive sampling strategies in synthetic and real ocean models

Master's thesis in Marine Technology
Supervisor: Martin Ludvigsen
Co-supervisor: Trygve O. Fossum
June 2021

Norwegian University of Science and Technology
Faculty of Engineering
Department of Marine Technology

NTNU

Norwegian University of
Science and Technology

NTNU Trondheim
Norwegian University of Science and Technology
Department of Marine Technology

<div align="center">

MASTER THESIS IN MARINE CYBERNETICS

SPRING 2021

FOR

STUD. TECH. Martin Skaugset

</div>

Title: Using Monte Carlo simulations to evaluate adaptive sampling strategies in synthetic and real ocean models

Work Description

The overall goal of this project, which is a part of the Nansen Legacy project, will be to map the oceanographic, biogeochemical and biological state of the Norwegian part of the Barents Sea and to deliver technologies that enhance or augment traditional measurements made from ships. These maps can be used to ensure that mobile sensor platforms collect the highest value data. This will further be used in developing adaptive algorithms for marine robots.

The main goal of this project is to develop and test an algorithm for adaptive behaviour for marine robots. In order to achieve adaptive behaviour, the robot need to model the marine environment, here Gaussian Process (GP) modelling is common. A GP is a collection of random variables which have joint Gaussian distributions. In this project GPs will be used achieve adaptive behaviour, as the robot needs to model the marine environment. The GP should model some ocean parameter like temperature, salinity or Chlorophyll-a. Different path planning algorithms should also be implemented, as the results from the adaptive behaviour should have a set of comparable simulations. For this an algorithm creating a path similar to a manually planned mission is sufficient. To verify the adaptive path planning algorithm, Monte Carlo simulations should be conducted.

Scope of work

1. Literature review focusing on
   a. Adaptive behavior for marine robots
   b. Collaborative behavior for marine robots
   c. Statistical modeling
2. Setup using LAUV, DUNE and the LAUV-simulator or Python.
3. Development and testing (in simulation) of a Gaussian Process model of an ocean parameter such as temperature, salinity or Chlorophyll-a.
4. Development and testing (in simulation) of an adaptive behavior algorithm for a single robotic platform.
5. Development of performance metrics to evaluate the performance of the adaptive behavior.

6. Compare the performance of the adaptive algorithm to that of other path planning algorithms, both for a synthetic ocean model and a model based on collected ocean data.

The report shall be written in English and edited as a research report including literature survey, description of mathematical models, description of control algorithms, simulation results, discussion and a conclusion including a proposal for further work. Source code should be provided online. It is supposed that the Department of Marine Technology, NTNU, can use the results freely in its research work, unless otherwise agreed upon, by referring to the student's work. The thesis should be submitted within June 24th.

Co-supervisor: Trygve O. Fossum

Supervisor: Martin Ludvigsen

Trondheim, 23.06.2021

Place, date

Martin Skaugset

Student

Martin Ludvigsen

Supervisor

Abstract

The Nansen Legacy project works towards enhancing traditional measurements made from boats. One of the approaches to this is using autonomous underwater vehicles (AUVs) for adaptive sampling. Using adaptive sampling over traditional measurement regimes imposes new challenges, and allow for optimisation of the sampling strategy. Based on theory from recent papers and simulations using Python, adaptive behaviour has been achieved.

This thesis presents theory which is needed to allow such algorithms to work efficiently. Using this theory, simulations of adaptive sampling have been performed. Using a Gaussian Process model to predict the surroundings is an important aspect of this work. These offer a practical probabilistic approach to modelling spatial dependent data and uncertainty.

To evaluate the performance of the adaptive algorithm, Monte Carlo simulations have been conducted. Monte Carlo simulations have not been performed for the other path planning algorithms, as these provide a deterministic path, only dependant on the uncertainty of the field. The overall performance using a synthetic ocean model has been compared to the performance using a SINMOD ocean model.

Sammendrag

Arven etter Nansen er et prosjekt som jobber for å forbedre tradisjonelle målinger gjort fra skip. En av måtene dette blir gjort på, er ved bruk av autonome undervannsfarkoster til adaptiv prøvetaking. Ved bruk av adaptiv prøvetaking i stedet for tradisjonelle prøvetakings-metoder kommer det nye utfordringer og samtidig åpner det for optimalisering av prøvetak-ingsmetoden. Basert på teori fra relevante artikler og simuleringer i Python, har en adaptiv prøvetakingsmetode blitt laget.

Denne oppgaven presenterer den nødvendige teorien for at slike algoritmer skal fungere effektivt. Ved bruk av denne teorien har adaptiv prøvetaking blitt gjennomført. Å bruke en gaussisk prosess modell for å modellere området omkring farkosten er en viktig del av dette arbeidet. Denne modellen gjør det mulig å modellere den romlige statstikken og gir et mål på usikkerhet.

For å evaluere ytelsen til den adaptive prøvetakingsmetoden har Monte Carlo simuleringer blitt gjennomført. Monte Carlo simuleringer har ikke blitt gjennomført for de andre kartleg-gingsalgorimene, siden disse gir en deterministisk rute, som bare er avhengig av usikker-heten i feltet.

Preface

This master thesis is written during the spring semester of 2021 of the 5th and final year of a master's degree in Marine Technology at the Department of Marine Technology, Norwegian University of Science and Techonolgy (NTNU). This thesis is on the topic of adaptive path planning and the work has been carried out at NTNU with a workload corresponding to 30 ECTS, where some of the conducted work is based on the work carried out during the Autumn of 2020, which was a project thesis corresponding to 7.5 ECTS.

I would like to express my gratitude to Prof. Martin Ludvigsen and Dr. Trygve O. Fossum, my supervisor and co-supervisor respectively. Thank you, for all your advise and encouragement.

Nomenclature

$\bar{x}$ Mean

δ Kronecker delta

ℓ characteristic length-scale of a process

ϵ Gaussian measurement noise

Γ Gamma function

μ Mean vector

μ_a Magnetic permability

ν Parameter of covariance

Σ Covariance matrix

σ Standard deviation

σ_a Electrical conductivity

θ Weighting factor

a Absorption of electromagnetic waves

n The total number of points in the grid

c   Speed of sound

F   Observation matrix

f   Frequency

S   Salinity

T   Temperature

z   Depth

Contents

List of figures

List of tables

Chapter 1

Introduction

1.1 Background

It is well known that most of the ocean is undiscovered. The Nansen Legacy project has as an overall goal to map the oceanographic, biogeochemical and biological state of the Norwegian part of the Barents Sea and to deliver technologies that enhance or augment traditional measurements made from ships.

To be able to efficiently perform operations in the ocean, it is important to have a good understanding of the environment. The capabilities within ocean observation are improving rapidly. Using ocean models combined with remote sensing and robotic elements allow for a better understanding of ocean dynamics. There are multiple essential factor connected to ocean mapping. Firstly, all measurements need to be carried using the vehicle itself for underwater operations. For these underwater operations there are few external sources available such as, GPS or stars for navigation or measurements of current velocity. In addition to this, detection of landmarks is also more difficult, as they might be few and far between. These factors combined provide challenges, which need to be solved in order to perform efficient mapping of the ocean.

Adaptive behaviour of a vehicle could be desirable for these types of challenges. Having a sensing autonomous agent which works towards finding the highest utility data, could provide a good foundation for further work. To achieve adaptive behaviour, an algorithm needs to be developed and tested. This algorithm needs to model the marine environment, in which Gaussian process (GP) modelling is common. Using this modelling to evaluate the proximity of the vehicles is essential to enable gathering of the highest utility samples.

There are multiple groups conducting research on cooperating marine vehicles. These types of systems impose more complex cooperation than other system types, due to challenges associated with underwater communication. These groups use different approaches, which can be applicable to this work of model-sharing and autonomy. Some examples of these applications are discussed in Leonard et al. (2007) and Pinto et al. (2018).

The goal for this thesis is to create an algorithm for conducting adaptive sampling for a single autonomous underwater vehicle (AUV), and develop a Gaussian process model. The adaptive sampling should utilise gradients to perform path planning. The Gaussian process

model is used for its powerful computational and practical properties. In addition to this, a goal for further work is to apply this work towards adaptive behaviour of cooperating marine vehicles.

1.2 Structure of report

This master thesis will focus on adaptive behaviour of a single AUV and is a continuation of the project thesis written during the Autumn of 2020. The second chapter presents work which is related to the work conducted throughout this thesis. The theoretical background for relevant concepts will be presented in the third chapter. Background which is useful for cooperating behaviour is also included in the second chapter, as a connection to possible further work. The fourth chapter will contain the method for the performed simulations, with a focus towards the implementation of the presented theory. The fifth chapter presents the results from the simulations, the sixth discusses these results, while also discussing the challenges which should be considered for further work. The last chapter will conclude the performed work and provide suggestions towards further work. .

1.3 Research question and methodology

To improve current traditional measurement strategies, adaptive behaviour could in many cases be beneficial. Adaptive behaviour is enabled through using a GP model, combined with the vehicles measurements.

This imposes several important questions. Firstly, how will different weightings between *exploration* and *exploitation* influence the behaviour and performance of such algorithms. Secondly, how does the performance of these algorithms compared to traditional measurement strategies, such as a manually planned operation. Lastly, is the performance of this algorithm impacted by use of a synthetically generate ocean model, compared to an ocean model based on real data.

Chapter 2

Related work

Using different ideas from fields like cooperating underwater robots and adaptive sampling requires a review of current literature on these topics. Related work on aspects which are important to these topics have been perform with different fields of focus. Overall Fossum (2019), Seto (2013) and Leonard et al. (2007) have made significant contributions to these topics.

Although there exist more work which could be useful, the focus of this section will be towards ocean observation, spatial statistics, cooperating systems, adaptive sampling and informed path planning, as these will all have direct relevance to this thesis.

2.1 Ocean observation

To be able to efficiently perform operations in the ocean, it is important to have a good understanding of the environment. The capabilities within ocean observation are improving rapidly. Using ocean models combined with remote sensing and robotic elements allow for a better understanding of ocean dynamics. Ocean observations are further discussed in Fossum (2019).

Within ocean observation, autonomous profiling floats have a been revolutionary development in oceanography, enabling global broad-scale observations of the ocean temperature, salinity, velocity and additional variables (Roemmich et al. 2004). Through monitoring of the ocean using the global Argo array, an improved coverage of the ocean both with respect to spatial and temporal coverage. The global Argo array had 1250 active profiling floats in 2004 and Riser et al. (2016) evaluates and attempts to provide an outline for the progression of the project, with the amount of active floats having increased to almost 3900.

There are many challenges connected to ocean sampling. The sampling conundrum in oceanography is explained in Fossum (2019). Challenges related to ocean sampling are described by Fossum (2019), including *Sparseness*, *Space-Time dependent environment*, *Proxy measurements*, *Sensing scales* and *Harsh environment*. These are all factors which need to be considered to varying degrees based on application and location.

2.2   Spatial statistics

Utilising statistical approaches for sampling, provides an important and powerful tool. Using the traditional model framework of GPs, analysing and modelling the ocean environment is discussed in Fossum (2019). Kroese and Botev (2013) provides the needed mathematical background to create different spatial processes, including generating a Gaussian process, using zero-mean Gaussian noise.

Illustrating GPs used for adaptive sampling by use of an AUV, is provided in Fossum (2019). Using simulated surface temperatures of a coastal area in Norway, a prior mean function has been created. Together with the mean, the covariance function was set to a *squared exponential* kernel. This example illustrates the use of GPs when considering ocean applications.

Required considerations for using GPs for ocean applications, are also discussed in Fossum (2019). The covariance will have have different properties, depending on the stationary properties. The ocean is an anisotropic non-stationary process, however, in practice stationarity is often assumed (Fossum 2019).

2.3   Cooperation between underwater vehicles

There are multiple groups doing research on cooperating marine vehicles. This imposes more complex cooperation than other system types. These groups use different approaches, to solve the challenges related these types of operations. Leonard et al. (2007) uses feedback control laws to stabilise the collective motion of a planar model of autonomous vehicles moving at a constant speed. Challenges related to underwater communication is discussed in greater detail both Leonard et al. (2007) and Seto (2013). Leonard et al. (2007) performs the communication of the gliders above surface via a central data hub, to avoid the limitations of underwater communication. The strategy used in Leonard et al. (2007) also allows for asyncronicity, as the gliders are not always able to surface simultaneously, which is important to consider for these types of operations. The experimental design when using communicating underwater vehicles needs to reflect the new challenges this imposes on the system. Handling of these challenges in discussed in Leonard et al. (2007).

2.4   Adaptive sampling

Different research towards adaptive sampling has been conducted. In Fossum (2019) adaptive sampling, refers to the act of making an intelligent and deliberate choice of when and where to gather data on the basis of informative and scientific metrics. Adaptive sampling thereby infers online decision making. With increasing computational capabilities, higher levels of autonomy has been introduced into the ocean domain. Varying approaches has both been considered and conducted, such as guidance and control theory, path planning, artificial intelligence and machine learning. The challenges connected to the ocean can be viewed as multi-disciplinary, as different aspects of the ocean domain is considered. This

includes biology, physical oceanography and other environmental scientists. For adaptive sampling, the space-time dependence of the ocean is essential, as different processes in the ocean have different spatio-temporal scales. The sampling of these different phenomena require different sampling approaches, used both different strategies for a moving sensor, but also different marine robotic platforms to provide the most optimal coverage (Fossum 2019).

Further for adaptive sampling Leonard et al. (2007) presents design and control of optimal trajectories for mobile sensor networks. The vehicles used in this application were self-directed gliders, which were used to sample dynamic ocean variables.

Leonard et al. (2007) also discusses the need for tools to better understand ocean dynamics. This include aspects like marine ecosystems and global climate. Both to gain a better understanding towards management and preparation of certain events.

2.5 Path planning

Path planning is a topic which is highly relevant to this thesis. Seto (2013) discussed various aspects of path planning, with a focus towards use for AUVs. Little research is done towards path planning for underwater vehicles compared to ground vehicles (Seto 2013). Although this is the case, many of the same concepts are applicable for path planning in underwater applications.

Informed path planning (IPP) is highly connected to adaptive sampling, and has been studied to different degrees. Olofsson et al. (2020) discusses combining IPP with multiple target tracking. The overall goal is to generate paths for a movable agent with sensing capabilities. These paths should be made according to maximising the overall value of the sampled data. IPP does however not aim to gain a total coverage, but rather to gain the highest utility data, with a limited budget. Studying IPPs can be divided into the optimisation algorithm and designing rewards functions. Both of these approaches aim to provide the optimal path for a given problem.

2.6 Thesis contribution

This thesis will focus mostly on adaptive sampling. Using a GP model to create a simulated model of an ocean temperature field, adaptive path planning has been established. The overall goal of this thesis is to provide insight into the possible improvements these types of behaviour could provide. A part of this work is creating not only the adaptive algorithm, but also creating a baseline for comparison. This baseline is a "lawn mower" pattern, which closely resembles the path chosen in a manually planned mission. Different performance metrics have been formulated to quantify the performance of the different implemented algorithms. To provide a better understanding of the behaviour of a adaptive sampling strategy, Monte Carlo simulations have been performed in order to better compare the overall performance to those of traditional measurement regimes.

Chapter 3

Theoretical background

This chapter will address the needed theoretical background for underwater operations.

3.1 Autonomy

The autonomy of a system is characterised at different levels, and autonomy will here be handled in four different levels.

1. Automatic operation
2. Management by consent
3. Management by exception
4. Fully autonomous

In automatic operation, the actions are performed automatically for well defined tasks, while a human operation handles higher level tasks. At the second level, management by consent, the system will handle some actions separate from humans, while for mission specific actions the system will recommend control actions, which need to be accepted by an operator. Management by exception goes one step further towards autonomy, where the system executes mission related functions when the reaction time is too short for human intervention. An operator may override, change plans or make corrections made by the system, whereas for certain actions the operator is called. The last level is fully autonomous which means the system performs all mission-related actions in unstructured environments, with the ability to plan and re-plan the mission. The operator can be informed about progress, but the system is independent of human operation. Vehicles like an AUV are considered fully autonomous due to being able to re-plan and perform a given mission from an initial given plan.

Autonomous systems differ from automatic systems in being able to use gathered information to alter an existing plan, whereas the automatic system is well suited for performing well defined task without human intervention. Autonomous systems are developed to perform complex tasks in unstructured environments with significant uncertainties. This can be implemented in various different ways, depending on application.

An important aspect of autonomous systems is situational awareness. Situational awareness can be divided into three separate levels. The first level is perception, which is that

the system should be able to perceive its surroundings. The second level is comprehension, where just sensing the surroundings is no longer enough. Being able to understand what the measurements mean is also important. The third and last level is projection, this includes being able to project the current situation forward in time, and to predict future challenges. Which level is needed is again dependant on the application. Autonomous systems can be achieved by combining reactive and deliberative control.

3.2 Underwater navigation

Underwater navigation is a challenge, which needs to be addressed to utilise collected data. Finding an accurate global position during underwater operations can be challenging, as there is normally little to no external infrastructure to rely on. Using an inertial measurement unit (IMU) for underwater navigation, provides an estimated position during operation. The IMU uses previous position combined with measurements of velocities and angular rate, a new position is estimated. However, if these types of systems are left unaided, the propagating uncertainty will increase without an upper limit. This rate of degradation will be governed by the accuracy of these measurements. To aid the IMU, typically a Doppler velocity log (DVL) will be used to directly measure the velocities of the vehicle. Together with these instruments, using acoustic positioning is also common. These types of systems use an acoustic signal from a known location to estimate the position of the vehicle. Using a combination of these instruments are in many applications beneficial. This is due to the acoustic signals being connected with relatively high levels of white noise compared to the IMU, thus providing an improved position estimate.

3.3 Underwater communication

Communication is necessary for cooperative operations, as transmission of data and information between the cooperating platforms is needed. Underwater communication is largely limited compared to ground and aerial applications. Radio waves are attenuated rapidly in water and for that reason many forms of communication are no longer suitable. Communication therefore requires different solutions underwater than for ground or aerial applications. Acoustic waves are commonly used, as these waves can travel over much longer distances underwater. These are several challenges associated to using acoustic signals. Firstly, the velocity of such signals given by equation (3.1), makes latency a problem. Secondly, this restricts the amount of data which can be exchanged. Compared to other methods of transferring data, underwater communication has a very low bandwidth. Using acoustic modems in underwater vehicles are therefore necessary to exchange information while submerged. The restrictions using acoustic modems can be offset by surfacing with the vehicle. When the vehicle no longer is under water, other means of communication can be utilised, such as Iridium communication and the global system for mobile communication (GSM).

$$c = 1449.2 + 4.6T - 0.055T^2 + 0.00029T^3 + (1.34 - 0.01T)(S - 35) + 0.016z \quad (3.1)$$

where T is the temperature in $C°$, S is the salinity measured in parts per thousand, z is the depth in m and c is the sound velocity in water in m/s.

3.3.1 Absorption of electromagnetic waves

Electromagnetic waves within the radio frequency range of the spectrum, will not propagate over longer distances due to absorption. The absorption is described by

$$a = \sqrt{\pi f \mu_a \sigma_a}, \tag{3.2}$$

where f is the frequency of the signal, μ_a is the magnetic permeability and σ_a is the electrical conductivity. As the electrical conductivity of sea water is higher than that of fresh water, the absorption is two orders of magnitude higher (Seto 2013).

3.4 Ocean observation

The studies of the ocean covers a multitude of scales and space-time (spatiotemporal) variability, including processes that are episodic. The primary platform for observation has been - and still is - ships. Although ships cannot completely be replaced by new sampling tools, newly developing technologies are becoming increasingly used (Fossum 2019).

A more synoptic ocean perspective has been enabled by the introduction of remote sensing and large-scale sensor networks. However, sensor measurements are still too far apart, or cannot resolve the necessary details (Fossum 2019). As previously stated the attenuation of radio waves restrict communication below the surface significantly, which is a part of the challenges connected to new remote sensing technology. Ocean model accuracy is not at the level at which it can replace *in-situ* observation (Lermusiaux et al. 2015). Hence, there are still a significant amount of unobserved water column, which the modelling of can be improved upon by combining various marine data sources. This would not only close the gap in coverage, but also in resolution. However, this would still not provide a detailed view of the entire environment and thereby only provide a quasi-synoptic coverage.

The challenges connected to ocean sampling, also called the sampling conundrum, is discussed by Fossum (2019). Summarised these challenges can be divided into:

- *Sparseness:* Observing the entire environment in detail both in terms of coverage and resolution, and is usually not possible thereby only providing a quasi-synoptic coverage.
- *Space-Time dependent environment:* The fundamental turbulent, heterogeneous, and episodic nature of the ocean makes observations time-dependent and sensitive to both location and scale. This will also affect the ability to keep up-to-date knowledge. Understanding and quantifying this influence is also challenging.
- *Proxy measurements:* Sensor observations are rarely able to acquire direct measurements of the process or quantity of interest. This introduces additional uncertainty. Some forms of instrumentation also affect the environment, which may cause instrument bias.
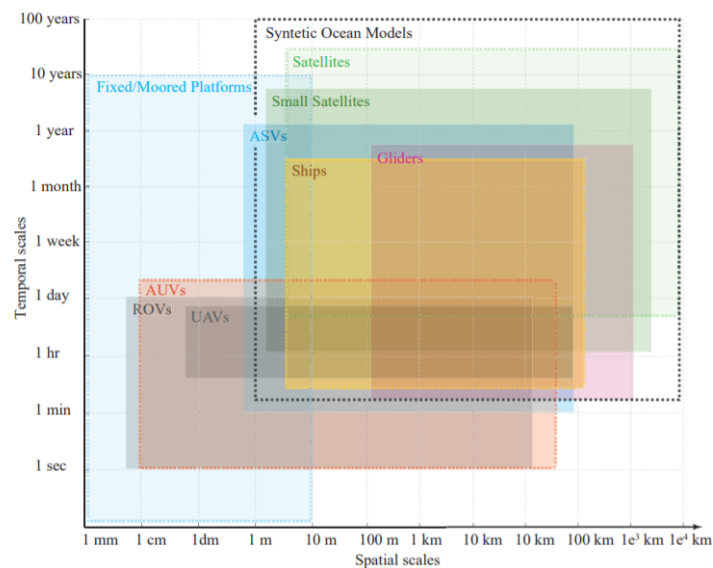
Figure 3.1: Common spatial and temporal characteristics for marine robotic platforms from Fossum (2019).

- *Sensing scales:* Using a multitude of different sensors to fill observation gaps, while avoiding undersampling makes cross-comparison complex.
- *Harsh environment:* Pressure, corrosion and bio-fouling affect all equipment that goes into the ocean. This causes the instruments to be both expensive and complex to install. Once the equipment is installed it will become subjected to varying loads and forces from phenomena such as waves, current and wind.

3.4.1 SINMOD ocean model

SINMOD is a numerical ocean model system which has been under continuous development at SINTEF since 1987. SINMOD connects and simulates physical and biological processes in the ocean. The model system is designed for use in both the northern and southern hemisphere. The Norwegian coast is represented through a series of model areas with a resolution down to 32 meters (Sintef n.d.).

SINMOD is a 3D hydrodynamic model, based on the Navier-Stokes equations. The model has a number of different uses, including research of physical and biological process in the ocean and current conditions used for analysis of marine installations and location analysis for aquaculture.

3.4.2 Application for synoptic ocean data sources

Using multiple different marine data sources is required to achieve the ambition of a more detailed understanding of the ocean. Data assimilation between heterogeneous marine data
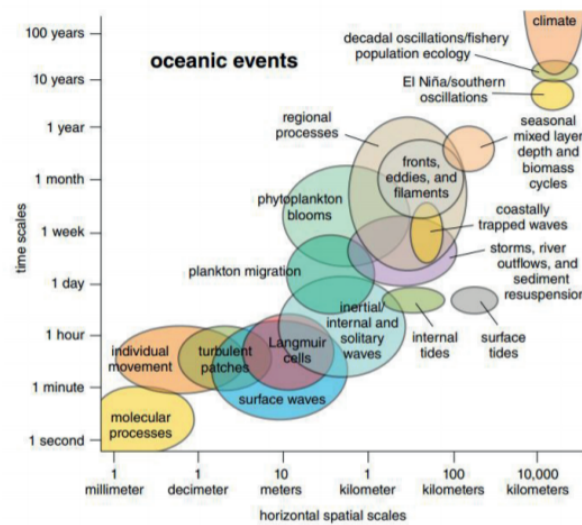
Figure 3.2: Some of the prominent oceanic processes and events from Schofield et al. (2013).

sources is also essential. Data assimilation is in itself a modelling techniques, which uses spares observations from marine data sources and platforms to constrain the dynamics of the model (Frolov 2007). A full assessment of the model accuracy is not possible, as this would require measurement of temporal and spatial gradients in the ocean far exceeding current practical capabilities (Curtin et al. 1993). Data from the surface is usually assimilated into operational models from remote sensing sources. It is therefore beneficial to evaluate model performance using observations from a range of different platforms. In addition to *hindcast* model validation and correction, information from *in situ* instrumentation can also improve near-real-time forecasting/*nowcasts* by assimilation of recent observations into the model (Fossum 2019).

3.5 Adaptive sampling

Adaptive sampling or data-driven sampling refers to the act of making an intelligent and deliberate choice of when and where to gather data on the basis of informative and scientific metrics, which infers online decision making (Fossum 2019). The aim of adaptive sampling is to efficiently fuse observations with prior knowledge to improve the utility of the agents actions and thereby enhancing the current strategy. An agent is defined in as: "*An agent is just something that acts*" (Russel et al. 2016). This means an agent describes an autonomous system which is able to perform actions.

Work conducted towards design and control of optimal trajectories for mobile sensor networks is discussed in Leonard et al. (2007). The vehicles used in this application were self-directed gliders, which were used to sample dynamic ocean variables.

The need for tools to better understand ocean dynamics is also discussed in Leonard et
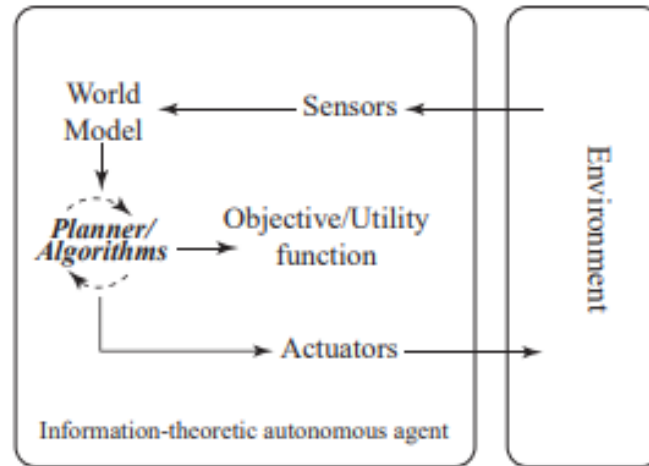
Figure 3.3: Information-theoretic autonomous agent architecture, following the $Sense \rightarrow Plan \rightarrow Act$ autonomy structure (Fossum 2019).

al. (2007). This include aspects like marine ecosystems and global climate. Both to gain a better understanding towards management and preparation for events such as red tides or El Niño.

3.5.1 Sampling optimisation

There are different approaches to sampling optimisation. These approaches can be divided into *coverage-* and/or *feature-based*. Optimisation can be classified as a problem deciding which locations to observe in order to efficiently decrease the uncertainty about a phenomena.

3.5.2 Exploration vs exploitation

The balance between exploration and exploitation is important when making decisions concerning gathering of information. Exploration concerns the collection of data which allow for leaning about the environment, while exploitation concerns gathering the most valuable information based on current knowledge. Being able to make the decision about which of these is the most important require a balance.

Decision-making is an important aspect towards balancing exploration and exploitation, both for single- and multi-agent approaches. Decision-making can be performed on multiple different levels in such a system. Six decision-making, planning and control levels of autonomy for unmanned underwater vehicles (UUV) are defined by Seto (2013). These range from *Direct control*, where the vehicle executes external commands without making decisions, to *Joint objective achievement*, where multiple objectives are balanced at once.

For cooperating systems there needs to be decision-making on different levels. The in-
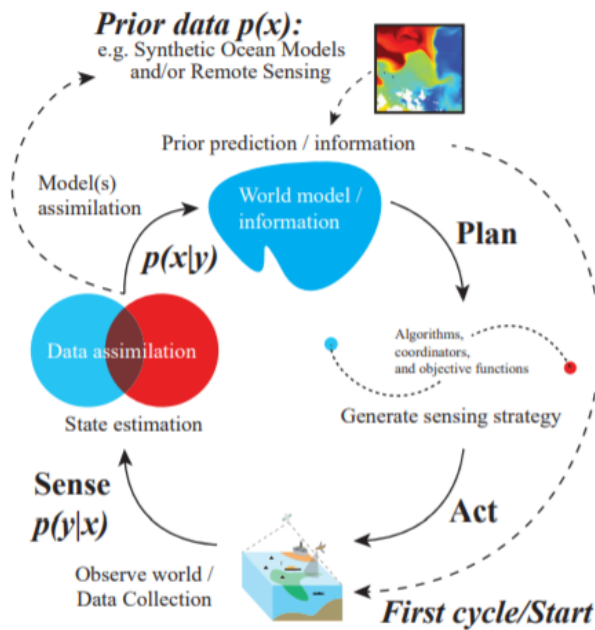
Figure 3.4: The data-driven/adaptive sampling cycle, where continuous assimilation and refinement of a sampling strategy follows the $Sense \rightarrow Plan \rightarrow Act$ control methodology from (Fossum 2019).

dividual agent needs to determine which actions are required to perform tasks which the agent have been assigned. In addition to this, a form of group decision-making is required, including dividing larger tasks into subtasks for a single agent.

3.5.3 Environmental modelling

To enable adaptive sampling, environmental modelling is fundamental. Without constructing an environmental model, the situational awareness of the agent will be lacking, and thereby directly influence the result. An model of the ocean rapidly becomes complex and current synthetic ocean models do not capture all complex features (Fossum 2019). Space and time variability are important factors in environmental modelling of the ocean, due to interaction of ocean processes. Space and time variability of the ocean is discussed in detail by Fossum (2019).

3.6 Cooperating systems

Due to restrictions in communication for underwater applications limited information can be exchanged between multiple vehicles, unless the vehicles are in close proximity or the path trajectories are planned for good communication, the communication will be significantly

limited. This concerns both the amount of data which can be exchanged and the frequency of interaction.

Cooperating systems allow for more efficient execution of various missions. These types of systems can be described in different ways. The systems are characterised by having multiple different physical systems (agents) performing actions to achieve a goal. This goal does not have to be the same for all agents as there might be subtasks to be performed to reach the overall goal.

Three main components to a system with cooperating agents are defined in Seto (2013).

1. A shared task view
2. A decision-making process
3. The behaviours that enable the agents to perform the tasks

These components are important to consider when creating a cooperating agents. Different approaches to these components can be applied, depending of the design criterion.

3.6.1 Shared task view

Having a shared task view is important to be able to construct cooperating systems. To achieve a shared task view between agents aspects which need to be addressed include:

1. The definition of the mission or problem the vehicles must address
2. Whatever tasks and subtasks may be necessary in order to complete it
3. All the information available relevant to the performance of the tasks and subtasks

Shared task view can be divided further into *goal representation* and *data management*. Ways to represent a goal are further discussed in Seto (2013), including restricting the amount of data, which is exchanged for underwater vehicles, while the internal representation of the goal can be different due to the restrictions in communication.

3.6.2 Information sharing

Sharing information between vehicles can be done using different approaches. If surfacing is applicable for the operation, communication can be done using the same type of infrastructure that is used for surface vehicles and aerial vehicles. When surfacing is not feasible, the communication must be done using acoustic signals. Using acoustic signals for communication can be challenging as the amount of data needs to be minimised, due to the low bandwidth of transmission. This gives data management a critical role in underwater operations with multiple agents.

3.6.3 Task allocation

Task allocation can be performed in multiple phases of and operation. In some cases allocation *a priori* can be performed. Assigning tasks *a priori* may however be difficult when the set of tasks is not well defined, then allocation could be performed during the mission, using specific algorithms to divide the problem.

In multi agent cooperation, utility-based approaches are common. These approaches use the expected utility of a set of actions to determine the highest utility actions for the agent. Using this method, weighting the relative benefit of different task allocations becomes possible, with a given strategy.

3.6.4   Negotiation

Negotiation between the agents is in some cases necessary to achieve the best action for all agents. When the group decisions rely on interest of the individual agents, reaching a consensus is necessary. Negotiation is difficult for underwater operations due to limited information being shared combined with not being able to have a up-to-data shared view, due to the transmission speed of information.

Negotiation could be performed if both vessels are surfacing, and then game theory becomes important. Finding a trade-off between utility of each individual agent, and thereby finding the optimal solution for the group. Game theory is further described in Koçkesen et al. (2007). To create a negotiation structure, most cooperative systems establish a hierarchy. The hierarchy is used to solve tie-breakers and improve consistency.

3.7   Spatial statistics

Spatial statistics is as previously mentioned, both a powerful and important tool in ocean modelling. Being able to learn from prior and current data to model the environment is an essential part of this work. Because ocean parameters are spatially correlated, the dependence needs to be managed by the spatial model. GPs are a common model framework for environmental sensing applications.

A perquisite for doing effective mission adaptation is to have accurate information about the spatial conditions, especially in highly dynamic environments, such as the ocean. To have a model of a spatial phenomenon is fundamental to be able to identify areas which are relevant according a sampling regime. This also imposes a formal measure of uncertainty, which is essential in providing meaningful information metrics for further use in adaptive sampling.

Using high fidelity numerical ocean models on board a robotic platforms is currently infeasible. This is due to the required numerical resolution, which translates into computational demands that are too high for the platform to manage (Fossum 2019).

As GPs provide multiple useful properties, which are especially useful in highly dynamic environments, such as an ocean environment. Using these properties allow for using an ocean model for simulations to verify the concept of adaptive sampling and cooperating systems. Using prior estimations combined with measured data, a GP model can be used to construct and update predictions (Fossum 2019).

There are different aspects which need to be considered when using GPs the ocean domain. The covariance of the GP, will have different properties depending on the stationary properties of the modelled field. The ocean is an anisotropic, non-stationary process, however, stationarity is in practice often assumed (Fossum 2019).

3.7.1 Gaussian processes

A GP is a stochastic process, such that every finite selection of those random variables have a Gaussian distribution. A Gaussian distribution is totally determined by its mean and variance. The GP is therefore defined by a mean vector, which contains means from the individual distributions, and a co-variance matrix consisting of covariances within the distribution.

The general Gaussian process can be written on the form

$$X \sim \mathcal{GP}(\vec{\mu}, \Sigma), \tag{3.3}$$

where $\vec{\mu}$ describes the mean vector and Σ describes the co-variance matrix. When making measurements this can be used to condition the process, to get a better estimate for other locations than the measured ones.

3.7.2 Conditioning a Gaussian process

The ability to condition a GP on is an important property. This means that the expected value and variance of the process can be reevaluated based on conditioning on measured data. The conditioning principle follows from the GP, following basic probability theory, once the mean and covariance are defined. After these have been established the GP can be used in a Bayesian setting where *Bayes' rule* is applicable. With given prior data, using the conditional probability, the posterior can be obtained using

$$p(\boldsymbol{x}|\boldsymbol{y}) = \frac{p(\boldsymbol{x}, \boldsymbol{y})}{p(\boldsymbol{y})} = \frac{p(\boldsymbol{x})p(\boldsymbol{y}|\boldsymbol{x})}{p(\boldsymbol{y})}. \tag{3.4}$$

Using Equation 3.4, where $p(\boldsymbol{x})$ is the prior model of $\boldsymbol{x}$, $p(\boldsymbol{y}|\boldsymbol{x})$ is the likelihood function and $p(\boldsymbol{y})$ is the marginal likelihood. The practical implication of this for GPs is that the posterior will also be Gaussian given that the prior and likelihoods are Gaussian. The expected value and variance using conditioning becomes

$$E(\boldsymbol{x}_A|\boldsymbol{x}_B) = \boldsymbol{\mu}_A + \Sigma_{A,B}\Sigma_B^{-1}(\boldsymbol{x}_B - \boldsymbol{\mu}_B), \tag{3.5}$$

$$Var(\boldsymbol{x}_A|\boldsymbol{x}_B) = \Sigma_A - \Sigma_{A,B}\Sigma_B^{-1}\Sigma_{B,A}. \tag{3.6}$$

This conditioning is based on two blocks of variables $\boldsymbol{x}_A = (x_{A,1}, ..., x_{A,n_A})$ and $\boldsymbol{x}_B = (x_{B,1}, ..., x_{B,n_B})$ and $n_A + n_B = n$. μ_A and μ_B are the means of the respective blocks.

Prior: $\boldsymbol{\mu} = \mu(s_i)$ for all locations $i = 1, \ldots, n$
Observation matrix: $\boldsymbol{F} = m \times n$ matrix with only 1 and 0 entries indicative of the survey design. m is the number of measurements or observations
Data: $\boldsymbol{y} = \boldsymbol{Fx} + \epsilon$, where $\boldsymbol{x}$ is a process (ocean model), with Gaussian measurement noise $\epsilon \sim \mathcal{N}(0, T)$ and $T = \tau^2 I$ where τ can be set manually
Covariance: $\Sigma = cov(s_i, s_j)$ for all locations i,j where $i = 1, \ldots, n$ and $j = 1, \ldots, n$

$$p(\textbf{prior}, \textbf{data}) = \mathcal{N}\left(\begin{bmatrix} \textbf{prior} \\ \textbf{data} \end{bmatrix}; \begin{bmatrix} \boldsymbol{\mu} \\ F\boldsymbol{\mu} \end{bmatrix}, \begin{bmatrix} \Sigma & \Sigma F^T \\ F\Sigma & F\Sigma F^T + T \end{bmatrix} \right) \tag{3.7}$$

Using Equation 3.4 to condition the Gaussian process, the conditional mean and covariance becomes:

$$\boldsymbol{\mu}_{posterior} = \boldsymbol{\mu} + \Sigma F^T (F\Sigma F^T + T)^{-1}(\boldsymbol{y} - F\boldsymbol{\mu}), \tag{3.8}$$

$$\Sigma_{posterior} = \Sigma - \Sigma F^T (F\Sigma F^T + T)^{-1}F\Sigma. \tag{3.9}$$

An important note to the conditioning of a Gaussian process is the term $(F\Sigma F^T + T)^{-1}$, which quickly becomes computationally expensive with the inverse of the covariance matrix. This can be a large drawback to using Gaussian process modelling for high dimensional problems. To counteract this drawback, sparse solutions can be used, such as presented by Bauer et al. (2017), Vanhatalo et al. (2010) and Krishnamoorthy et al. (2013).

3.7.3 Covariance

The covariance matrix of the GP can be described by covariance matrix Σ where Σ_{ij} is the covariance of elements i, j in the matrix.

$$\Sigma = \begin{bmatrix} \Sigma_{11} & ... & \Sigma_{1n} \\ \vdots & \ddots & \vdots \\ \Sigma_{n1} & ... & \Sigma_{nn} \end{bmatrix} \tag{3.10}$$

Covariance will normally be modelled using a covariance function, a *kernel*. Kernel functions are described further in Fossum (2019). Letting $\mathcal{K}(i, j)$ denote the kernel function, the covariance becomes $\Sigma_{i,j} = \sigma_i \sigma_j \mathcal{K}(i, j)$. It can be seen that for different correlation distances the smoothness of the kernel function will change (Fossum 2019). Using different formulations of the kernel function will also affect the smoothness of the kernel function, shown in Figure 3.5.

3.7.4 Useful properties of a Gaussian process

There are multiple different properties of a GP which can be useful. Firstly the combination of modelling and computational properties is important. GPs allow for combining models with computational tractability, allowing models to be run on board the vehicle. Secondly, the Gaussian distribution is described only by its mean and covariance. Having an estimate for a covariance function, the GP can be used with sparse prior data. In addition to these factors, the GP allows for quantification of the uncertainty of the process.

3.7.5 Creating a Gaussian process

To create a Gaussian process, the underlying assumptions of the Gaussian distribution needs to be fulfilled. As previously stated, a Gaussian process is only determined by its mean and covariance. To ensure this, a Gaussian process need to be created with this in mind.

A Gaussian process can be generate by Kroese and Botev (2013):

1. *Construct the mean vector $\mu = (\mu_1, \ldots, \mu_n)^T$ and covariance matrix $\Sigma = (\Sigma_{i,j})$ by setting $\mu_i = \tilde{\mu}_{t_i}$, $i = 1, \ldots, n$ and $\Sigma_{ij} = \tilde{\Sigma}_{t_i,t_j}$, $i, j = 1, \ldots, n$*
2. *Find a square root A of Σ, so that $\Sigma = AA^T$*
3. *Generate $(Z_1, \ldots, Z_n) \sim \mathcal{N}(0,1)$. Let $\mathbf{Z} = (Z_1, \ldots, Z_n)^T$*
4. *Output $\mathbf{X} = \mu + A\mathbf{Z}$*

Using the Cholesky's square root method, it is always possible to find a real-valued lower triangular matrix A, such that $\Sigma = AA^\top$ from Kroese and Botev (2013).

3.7.6 Kernel functions

The kernel function is fundamental to using GPs in different applications. The kernel function is applied to each data instance to be able to map original non-linear features to higher-dimensional space. This space is called a feature space, in which the non-linear features are separable. This technique is called to "kernel trick", and can be particularly valuable if the feature vectors are more challenging to compute than the kernel.

Formulating kernel functions which can be used in different applications can be difficult. They might require a good mathematical understanding of the problem at hand. With this in mind, choosing the correct kernel function might not be easy, while finding an adequate solution might in some cases be sufficient. Multiple different kernels can be used to test which provide the best estimate for a specific model, given that the underlying pattern is known. If the underlying pattern is unknown, evaluating the kernel function becomes more difficult, and again requires a good mathematical understanding of the problem to evaluate the output.

Some common kernel functions can be written on the form

$$\mathcal{K}_{Matern}(\boldsymbol{x}, \boldsymbol{x}') = \frac{2^{1-\nu}}{\Gamma(\nu)} \left(\frac{\sqrt{2\nu}|d|}{\ell} \right)^{\nu} K_{\nu} \left(\frac{\sqrt{2\nu}|d|}{\ell} \right), \tag{3.11}$$

$$\mathcal{K}_{GN}(\boldsymbol{x}, \boldsymbol{x}') = \sigma^2 \delta_{x,x'}, \tag{3.12}$$

$$\mathcal{K}_{SE}(\boldsymbol{x}, \boldsymbol{x}') = \exp -\frac{|d|^2}{2\ell^2}. \tag{3.13}$$

Shown in these equations are the kernels for Matern-, Gaussian noise- and Squared exponential functions. ℓ denotes the characteristic length-scale of the process, δ is the Kronecker delta and $d = x - x'$.
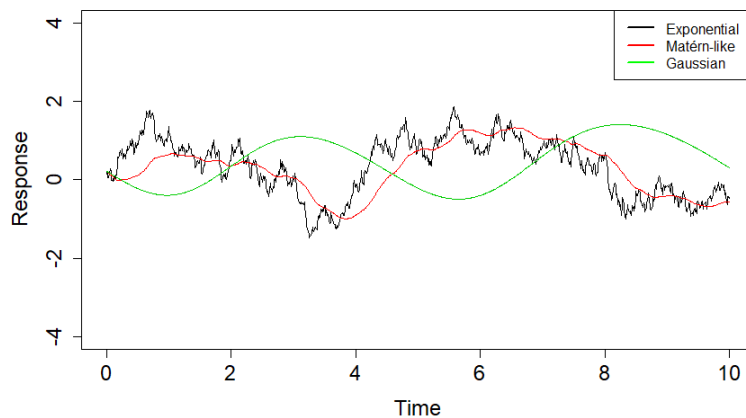
Figure 3.5: Realisations of three different kernel functions in R.

3.8   Path planning

Path planning is an important topic towards adaptive sampling, concerning the problem of finding a path between two points. This does not include fundamental movements of the vehicle, which is included in motion planning, but rather focuses on providing a path from A to B. There are many different approaches to finding a path. Some of these approaches, like the A-star algorithm, aim to find an optimal path between the points, while others aim to find a solution to the path planning problem, without consideration for the optimality of the solution. Various aspects of path planning, with a focus towards use for AUVs are discussed by Seto (2013). Little research is performed towards path planning for underwater vehicles compared to ground vehicles (Seto 2013). Although this is the case, many of the same concepts are applicable for path planning in underwater applications.

The path planning problem needs to define some fundamental terms as described by Seto (2013). Path planning will normally be in one or multiple of the areas: *Navigation*, *Coverage*, *Localisation* and *Mapping*. Navigation considers the problem of finding a collision-free path for an environment containing obstacles. The goal of path planning for coverage is to measure every point in the environment. Localisation is to localise the robot within an environment. Lastly, the goal of mapping is to gain knowledge which was previously unknown about an environment. Localisation and mapping may for some applications combined into *Simultaneous Localisation and Mapping* (SLAM).

When discussing path planning algorithms, some terms need to established in order to compare different approaches.

- *Optimality:* Does the algorithm find the optimal solution to the given problem?
- *Completeness:* Will the algorithm find a solution, if a solution exists?
- *Offline planning:* All knowledge of the environment is known *a priori* and the plan can therefore be planned completely before execution.

- *Online planning:* Constructing the plan incrementally during execution.
- *Sensor-based planning:* Sensor measurements are processed and used for online planning.
- *Deliberative:* The cycle of sensing, then planning, then acting, is created in each iteration.
- *Reactive:* Using information from sensor measurements to reach the goal, without the need for a representation of the entire environment.

Informed path planning (IPP) is highly associated to adaptive sampling, and has been studied to different degrees. Combining IPP with multiple target tracking is discussed by Olofsson et al. (2020). The overall goal is to generate paths for a movable agent with sensing capabilities. These paths should be made according to maximising the overall value of the sampled data. However, IPP does not aim to gain a total coverage, but rather to gain the highest utility data, with a limited budget. Studying IPP can be divided into the optimisation algorithm and designing rewards functions. Both of these approaches aim to provide the optimal path for a given problem.

3.8.1 Myopic (greedy) vs Non-myopic/synoptic sampling

Assumptions and simplifications are often needed to obtain a feasible solution when the complexity of studying spatial sampling in a dynamic (non-stationary) system is considered (Fossum 2019). Various approaches can therefore be considered. One of these approaches is to discretise the problem into a graph structure, built by assigning measurement locations within the graph. This allows for evaluating the graph along the graphs edges. Evaluation can be *myopic* (greedy), using a fixed and usually short planning/evaluation horizon, or be more synoptic, planning over several sequential steps (*non-myopic*). One important aspect to consider is that greedy strategies are subject to the *local minima* problem of optimisation. Non-myopic schemes avoid this by looking further ahead (several sampling steps) and more elaborate searching criteria. However, these is a fundamental difficulty specifically related to environmental sampling in the ocean. Namely the face that it is difficult to attain and maintain synoptic up-to-date knowledge, this is especially important for the water column. Planning ahead only makes sense if you can trust the quality of the information (Fossum 2019).

The work from Low et al. (2008) showed a sequential approach for multiple robots. This work incorporated assimilation of newly gathered data using dynamic programming, GPs and posterior variances and entropy as the performance metrics. The same metric and mutual information was later used by Binney et al. (2010), adapted to a recursive greedy approach, with a finite horizon. Trying to move away greedy and myopic strategies introduces issues with scalability, running time and computational load. These typically arise from increasing dimensionality in the problem space, such as increasing the graph size or resolution. Markov properties and Monte Carlo approaches are typically used to alleviate the computational burden and find feasible solutions. Branch and bound methods have also been used to limit dimensionality growth. Greedy approaches avoid this problem entirely by using a limited look-ahead, sacrificing optimality and/or completeness.

3.8.2   Path planning algorithms

Once a map of the surrounding environment is built, and the vehicle has been able to locate itself, the high-level task of path planning must be achieved in order for the platform to complete its mission. There are many different solutions to the path planning problem, using various algorithms. These algorithms calculates waypoint for the vehicle, which could be calculated one or several at a time, or even completely preplanned. By only calculating one waypoint at a time the algorithm only considered the implication of its current action, and not its effect on future actions.

Dijkstra's algorithm

Dijkstra's algorithm is the most common example of a shortest path algorithm. The main idea of this algorithm is to explore path by cost, and then keep track of which nodes have been visited, to evaluate the shortest path between two points. Visited nodes are stored in a priority queue, whereas the cost of reaching the nodes is also stored for further use.

A-star

The A-star algorithm is considered as a "best-first search", and can be implemented in different manners depending on application. With a known position of a goal, the A-star algorithm uses a heuristic function to evaluate which nodes to explore. This leads to fewer nodes being explored, and thereby reducing time complexity. Under the restriction that the heuristic is consistent A-star will find the optimal solution in a graph search. A consistent heuristic can be described as a heuristic function, which for all nodes in the graph, the sum of the path cost and the heuristic value, reflects the actual distance between the points. This can be described by the equation

$$h(n) \leq c(n, a, n') + h(n'), \tag{3.14}$$

where $h(n)$ is the heuristic function, $c(n, a, n')$ is the path cost between point n and n', where n' is a successor of n, and a is an action.

   The first step to ensuring optimality for an A-star algorithm is to find that $h(n)$ is consistent and that values along any path in $f(n)$ is non decreasing. This can be described by the equation

$$f(n') = g(n') + h(n') = g(n) + c(n, a, n') + h(n') \geq g(n) + h(n) = f(n). \tag{3.15}$$

Entropy-based path planning

Entropy within information theory represents the average level of information or uncertainty inherent in the a variables possible outcomes. Said differently entropy is the expected value of the information content of a discrete random variable. Entropy is not only about the number of possible outcomes, but also about their frequency (Learned-Miller 2013).

With a discrete random variable X, with possible outcomes $x_1, \ldots, x_n$ which occur with probability $P(x_1), \ldots, P(x_n)$, the entropy of X is formally defined as

$$H(X) = -\sum_{i=1}^{n} p_i \log p_i. \tag{3.16}$$

Planning non-myopic observation paths $x_{1:n}^*$ with maximum entropy is described by Cao et al. (2013):

$$x_{1:n}^* = argmax H(Z_{x_{1:n}}). \tag{3.17}$$

Uncertainty-based path planning

Uncertainty based path planning aims to decrease the uncertainty of the ocean model. This can be executed in different manners. A subset $\mathcal{A}$ is the potential sampling locations compatible with logistic constraints such as number of platforms, available time, depth rating, etc (Fossum 2019). The optimal subset of sampling locations $\mathcal{A}^*$, that maximises reduction of uncertainty can be expressed as

$$\mathcal{A}_V^* = \underset{\mathcal{A} \subseteq \mathcal{V}}{argmax} \frac{1}{N}(tr(\Sigma_0) - tr(\Sigma_{s|\mathcal{A}})), \tag{3.18}$$

where $tr(\cdot)$ is the trace of a matrix and N is the total number of possible measurement locations. This criterion, using trace of the matrix, is also known under the name of Bayesian A-*optimality* (Fossum 2019). As the covariance matrix consists of variances of the locations in a grid along the diagonal, using this criterion with the trace of the matrix aims to choose the sampling location which reduces the overall uncertainty of the field by the largest margin.

Using uncertainty on its own to perform path planning, the path can be calculated prior to the operation as the algorithm takes no input from the sampled field, and only calculates the waypoints based on the on-board model of the environment.

To expand this algorithm, input from the underlying field needs to be considered, thereby making a *data-driven criterion*. As opposed to the *uncertainty-driven criterion*, using measured data allows for reducing the uncertainty of a random field, while increasing the utility of each measurement. Using observations, the strategy is no longer deterministic as the observations depend directly on a sampled random field. The path chosen by the vehicle is therefore deterministic for a given randomly generated field, but as the total field is not known prior to operation, the path cannot be calculated *a priori*.

Including measurements can be handled by utilising the magnitude, or the gradient of the sampled data. This can be expressed by:

$$\mathcal{A}_V^* = \underset{\mathcal{A} \subseteq \mathcal{V}}{argmax} \theta_1 \frac{1}{N}(tr(\Sigma_0) - tr(\Sigma_{s|\mathcal{A}}) + \theta_2 \frac{1}{N} \nabla(\mu(\mathcal{A})). \tag{3.19}$$

θ_1 and θ_2 are factors which can be used to balance the terms between *Exploration* and *Exploitation*. There are different approaches to find the balance between these factors, and this will highly depend on the goal of the operation. For some applications the balance between these factors could change during operation, to increase exploitation when the vehicle has entered some area of particular interest.

Mutual information

Mutual information is a measure of the mutual dependence of two random variables. From Learned-Miller (2013), mutual information is formally defined as

$$I(X;Y) = \sum_{x \in \mathcal{X}} \sum_{y \in \mathcal{Y}} P(x,y) \frac{P(x,y)}{P(x)P(y)}. \tag{3.20}$$

In this definition $P(x)$ and $P(Y)$ are the *marginal distributions* of X and Y, obtained through a marginalisation process. This means gathering information about a variable also obtains information about a second variable. Mutual information path planning build on the concept of entropy-based path planning, and can also be defined as

$$MI(\mathcal{A}) \equiv H(\mathbf{x}_{\mathcal{V}/\mathcal{A}}) - H(\mathbf{x}_{\mathcal{V}/\mathcal{A}} | \mathbf{x}_{\mathcal{A}}). \tag{3.21}$$

The optimal subset of sampling locations $\mathcal{A}^*$, with maximal mutual information is then

$$\mathcal{A}^*_{MI} = \underset{\mathcal{A} \subseteq \mathcal{V}}{arg\,max} \frac{1}{2} \log((2\pi \cdot e)^n (det(\Sigma_{\mathcal{V}/\mathcal{A}}) - det(\Sigma_{\mathcal{V}/\mathcal{A}|\mathcal{A}})), \tag{3.22}$$

where $\Sigma_{\mathcal{V}/\mathcal{A}|\mathcal{A}}$ can be inferred from equation (3.9). By using the determinant of the matrix the covariance of the measurement locations is considered. This is in contrast to using the trace of the matrix, which will only consider the variance of the measured locations.

3.8.3 Performance metrics

To evaluate the results from the simulations, some performance metrics need to be formulated. To evaluate the performance between the utilities, one can either use root mean square error (RMSE) or $\mathbf{R}^2$. This statistic computes the percentage of prior variance which has been captured by the observations as: To quantify the performance of different path planning algorithms, some performance metrics needs to be formulated. From Fossum (2019) the performance metrics of $\mathbf{R}^2$ and RMSE are used. These can be defined as

$$\mathbf{R}^2 = 100 \cdot (1 - \frac{\Sigma_{posterior}}{\Sigma_{prior}}), \tag{3.23}$$

$$RMSE = \sqrt{\frac{1}{n} \sum_{i=1}^{n} (f_i - o_i)}, \tag{3.24}$$

where n is the total number of points in the grid, f_i are the forecasts and o_i are the observed measurements.

In addition to these criterion, it is necessary to define some metric, which provides information about the balance between exploration and exploitation. Where $\mathbf{R}^2$ provides a value for the overall coverage of the field, the RMSE does not fully provide a metric for the "usefulness" of the measurements. The value of the RMSE could be largely influenced by $\mathbf{R}^2$ if the estimation of the field prior to operation is not sufficiently close to the underlying
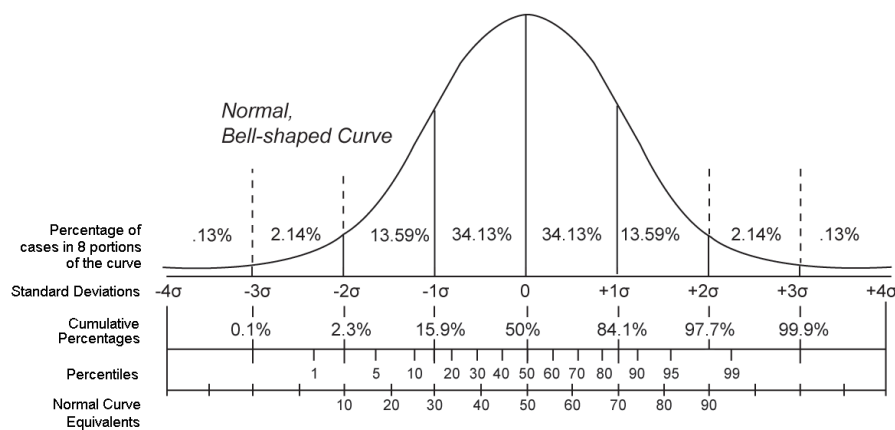
Figure 3.6: Visualisation of percentiles of data from *Percentile rank* (2021).

values of the field. Therefore, using time spent above certain percentiles of temperature, salinity or Chlorophyll-a can better provide the desired information. The exclusive percentile of a data set is a score below which a given percentage of scores in its frequency distribution fall. The inclusive percentile contains scores at or below the given percentage.

3.8.4 Application to AUVs

To be able to complete mission objectives, an AUV needs to calculate a path. This includes generating waypoints, which are then handled by an outer loop reference, that assumes the inner loop controller is able to stabilise the vehicle and thereby track the reference. These waypoints can be calculated *a priori* or during operation. Normally for seabed surveys these waypoints will be predetermined according to the area where the survey is conducted. Most of the research conducted has studied ground robotics, indicating the different approaches needed to be evaluated to find the feasibility for applying them to AUV planning.

3.9 Monte Carlo simulations

Monte Carlo simulation is a type of simulation which relies on repeated random sampling, to obtain numerical results and statistical analysis to compare the results. Typical uses of the Monte Carlo method (MCM) are *sampling*, *estimation* and *optimisation* (Kroese, Brereton et al. 2014). In sampling, the objective is to gather information about a random object by observing many realisations of it. For estimation MCM is used to estimate certain numerical quantities related to a simulation model. MCM is considered a powerful tool for optimisation of complicated objective functions. In many applications these functions are deterministic, and randomness is introduced artificially in order to efficiently search the domain of the objective function. The method of simulation is very closely related to random experiments, for which the result is not known in advance (Raychaudhuri 2008). Monte Carlo simulations have different application areas presented by Raychaudhuri (2008) and Glasserman (2003).

There are multiple reasons to why Monte Carlo techniques are popular. Monte Carlo techniques are normally simple, flexible and scalable. When applied to physical systems, the complexity of the model can be reduced to a set of basic events and interactions. This allows efficient implementation on a computer. Monte Carlo algorithms are also eminently parallelisable, as various parts can be run independently. This allows for parts to run on different computers and/or processors, and therefore significantly reducing the computational time. The inherent randomness of the MCM is not only essential for the simulation of real life random systems. It is also of great benefit for deterministic numerical computation. An example of this is when employed for randomised optimisation. The randomness permits stochastic algorithms to naturally escape local optima - enabling better exploration of the search space - a quality which is not usually shared by their deterministic counterparts (Kroese, Brereton et al. 2014).

3.9.1 Formulas for statistical analysis

To evaluate the output from the Monte Carlo simulations, some formulas for statistical analysis are needed. Using Monte Carlo simulation, these equations are estimates of the complete population based on the simulated sample.

Mean ($\bar{x}$) is described by

$$\bar{x} = \frac{1}{n} \sum_i x_i. \tag{3.25}$$

Standard deviation (σ) and **variance** (σ^2) are described by

$$\sigma = \sqrt{\frac{1}{N} \sum_i (x_i - \bar{x})}, \tag{3.26}$$

$$\sigma^2 = \frac{1}{N} \sum_i (x_i - \bar{x}). \tag{3.27}$$

The **skewness** of the sample, which is a measurement of the asymmetry of the sample, is described by

$$Skewness = \frac{\sum_i (x_i - \bar{x})^3}{(N-1) \cdot s^3}. \tag{3.28}$$

The **kurtosis**, like skewness describes the shape of the collected sample. Mathematically this is expressed by

$$Kurtosis = \frac{\sum_i (x_i - \bar{x}i)^4}{(N-1) \cdot s^4} - 3. \tag{3.29}$$

The standard error of a sample (SEM) is used to describe how precise the mean of the sample is as an estimate of the true mean of the population. SEM in contrast to the standard deviation, deceases by increasing sample size n, which does in general not have a trend with increasing sample size.

$$MeanStd.Error = \frac{\sigma}{\sqrt{n}} \tag{3.30}$$

Chapter 4

Method

4.1 Simulation model

The simulation model has been created using *python*. Due to the limitations in simulation capabilities using the LSTS Toolchain, an independent model has been created. The LSTS toolchain is an open-source software toolchain, developed by Underwater Systems and Technology Laboratory (LSTS) in Porto. The most important limiting factor in the LSTS toolchain is the need for simulations to be conducted in real-time. Conducting simulations in real-time is not a feasible solution to test an adaptive path planning strategy, in many different simulated Gaussian fields. For Monte Carlo simulations, this would imply a simulation time up to 6000 hours per simulation set up, when assuming 1000 simulations and six hours of operation time per simulation was needed.

4.1.1 Set up

The simulation model consists of two main components, the model of the AUV behaviour and a Gaussian process model. The Gaussian process model is used in two different instances. One to create the synthetic temperature field, in which the AUV samples data, and one as a sub module of the AUV to allow for adaptive behaviour, and path planning in general.

4.2 Implementation

To implement the presented theory, *python* has been used. The simulation model consists mainly of two classes. One class for Gaussian modelling and one class to represent the AUV. For simulations without an ocean model based on real data, a synthetic ocean model is created based on equations presented in subsection 3.7.5. The AUV is initialised with a temperature field containing only temperatures of 5 degrees Celsius. As the AUV explores new locations, a measurement is used to update the temperature prediction of the AUV according to equation (3.8).

Discretisation of a 50×50 grid has been performed. This creates $50 \times 50 = 2500$ different sampling locations for the AUV.

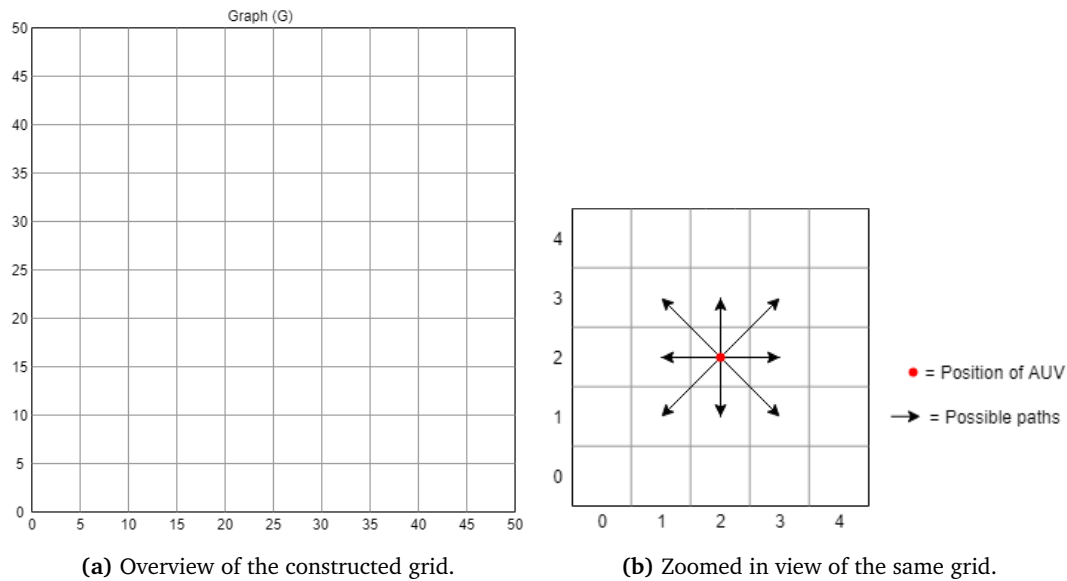**(a)** Overview of the constructed grid.　　　　**(b)** Zoomed in view of the same grid.

Figure 4.1: Representation of the constructed grid.

The AUV class consists of 3 main functions, with their required subfunctions. The first function stores measured data to the AUV. The second function calculates the next waypoint in the constructed graph. The third function is used to move the AUV within the graph. To calculate the next waypoint different path planning algorithms have been implemented. Using different criterion, the desired waypoint of the AUV is calculated. To allow for path planning based on the Gaussian model, an instance of the GP class is created within the AUV class. This simulates the on board Gaussian model used for evaluation of the surroundings of the AUV. The overall structure of the implementation is presented in Figure 4.2

Algorithm 1: AUV planning sequence

Initialise GP
for *iteration* **in** *number of iterations* **do**
    Save temperature of current position
    Calculate waypoint
    Move to waypoint in graph G
end

4.3   Gaussian processes

The Gaussian process model has been made using python, using a model provided by Trygve O. Fossum at NTNU. Some modifications were needed to expand the functionality of the model. As many processes can be described by a combination of Gaussian distributions, the surroundings of the vehicles can be modelled using GPs. This is performed by creating a
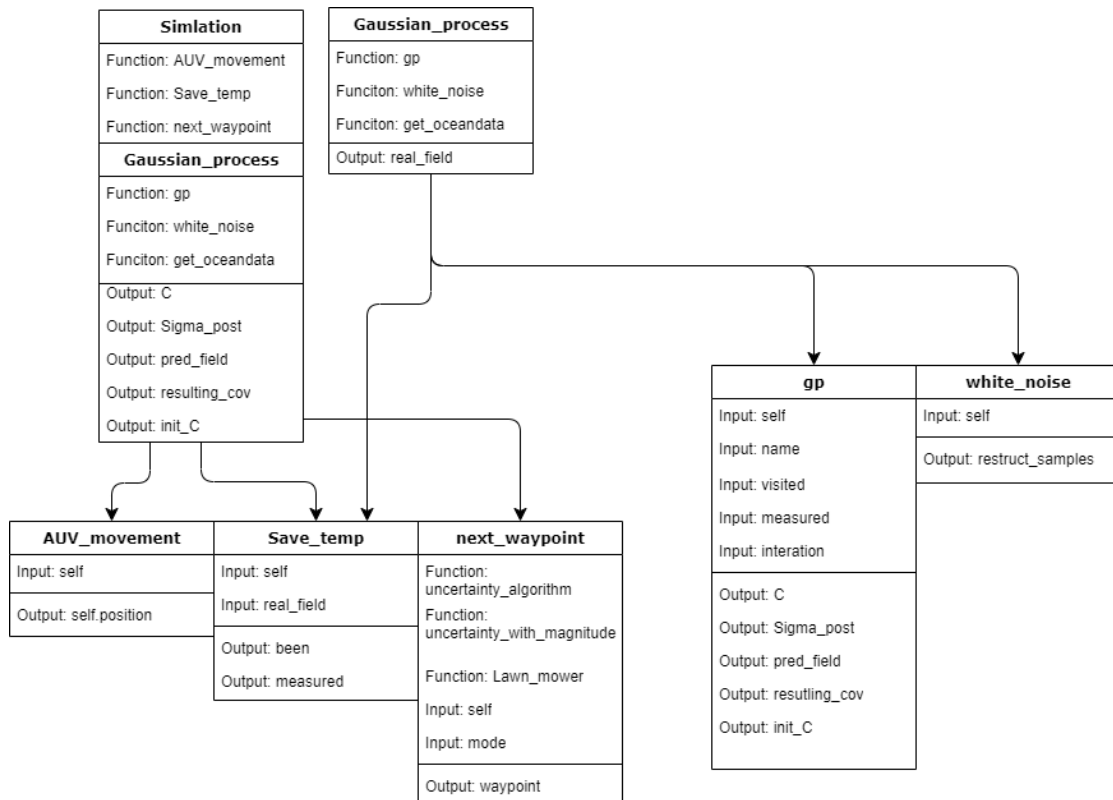
Figure 4.2: Overview of the program structure.

set of prediction locations, combined with a set of measured locations. Then constructing a covariance matrix for these locations, and use regression to generate a prior mean. Using this prior combined with measured data, a prediction can be made.

From the Gaussian process model the covariance matrix and the mean have been kept. These are used enable path planning for the AUV. Using the posterior mean from the GP model, a posterior prediction of the fields temperature is created. The hyperparameters of the Gaussian process model are design parameters for the variance and a correlation length, which have been set to 0.04 and 70, respectively.

For a realistic simulation the hyperparameters of the GP model aboard the AUV should be set differently to those used to create the synthetic ocean model. This is because finding the exact parameters for a real temperature field would generally not be possible to determine. The design parameter and correlation length of a true field are also more complex due to anisotropy.

4.3.1 Generating a Gaussian field

For simulations without input of an ocean model based on real collected data, a synthetic ocean model is created. Provided a design parameter for variance and correlation distance

---

Algorithm 2: Calculation of next waypoint

Initialise GP
Establish neighbouring points **in** graph G
for *i,j* **in** *neighbouring points* **do**
 if *Point is outside of grid* **then**
  | continue
 end
 if *Point has been visited* **then**
  | continue
 end
 Set neighbouring point to visited
 Calculate the corresponding covariance matrices
 Reset neighbouring point
 Evaluate objective function
 if *Objective function > Previous maximum* **then**
  | Set waypoint to this neighbouring point
  | Save value of objective function
 end
end

---

combined with Gaussian white noise a Gaussian field is created.

This model becomes an instance of the GP class, and becomes input into the AUV. From this point the AUV is able to move within the constructed grid and measure the temperatures in the synthetic ocean model. The synthetically generate ocean models, have a mean value of $9°C$, where as the initial temperature prediction aboard the AUV has been set to $5°C$.

In subsection 3.7.2 the covariance of the Gaussian measurement noise $T = \tau^2 I$. τ has been set to 0.005.

4.3.2 Kernel function

To create the covariance matrix, a kernel function is applied. The used kernel function is a modified version of the square exponential kernel function.

$$\mathcal{K} = \sigma \cdot e^{-3\frac{1}{l}} \cdot \sqrt{y - y'} \qquad (4.1)$$

Where σ is the design parameter for the variance, l is the correlation length and y is a given point and y' is another point within the grid. In initial simulations the design parameters has been set to $\sigma = 0.04$ and $l = 70$. These values have been used throughout simulations. Other values of the design parameters have been used in order to evaluate the GP generation.

4.4   Path planning

Creating a grid enables path planning to be performed as explained in section 3.8. Different path planning algorithms have been used to create a better understanding of each algorithms performance. Using only the uncertainty of the field path planning is performed based on criteria presented in section 3.8.2.

Basing the path planning algorithm only on the uncertainty of the field, the path of the vehicle can be calculated *a priori* as it takes no input from the sampled field. To achieve adaptive behaviour this needs to be expanded to include input from the sampled field. This can be implemented by including the magnitude of the measurements, or the sampled gradient. Using the magnitude combined with uncertainty is presented in Equation 3.19.

To perform path planning for the AUV, three different algorithms have been used. Firstly, an algorithm which causes the AUV to follow a lawn mower-like pattern to establish a baseline for the other path planning algorithms. Secondly, an algorithm based on the uncertainty from the GP model is used. Using the prior and posterior covariance matrices from the GP model allows for planning a path, which with each iteration of the AUV movement, will move to the location, which decreases the overall uncertainty of the field the most. Lastly, a path planning algorithm based on the same uncertainty from the GP model combined with the usage of predicted magnitude of the measurement has been used. When combining uncertainty with magnitude, the balance between exploration and exploitation is important. Using equation (3.19), different weighting between θ_1 and θ_2 has been considered.

Three different scenarios have been considered, using different weighting θ_1 and θ_2, where θ_2 has been defined as $\theta_2 = 1 - \theta_1$ and $\theta_1 \in [0, 1]$. The chosen values of θ_1 and θ_2 are presented in Table 4.1.

Table 4.1: Weighing parameters used in the different simulation runs.

Simulation run	θ_1	θ_2
1	0.9	0.1
2	0.8	0.12
3	0.6	0.6
4	0.5	0.5

4.5   Performance metrics

To evaluate the results from the simulations, some performance metrics need to be formulated. To evaluate the performance between the utilities, one can either use RMSE or $\mathbf{R}^2$. This statistic computes the percentage of prior variance which has been captured by the observations as: Thereby calculating the overall coverage by comparing the variance of all grid cells prior and post operation. The root-mean square error or RMSE can be calculated according to:

Where n is the total number of points in the grid, f_i are the forecasts and o_i are the observed measurements.

To establish a baseline for the simulation results, a lawn mower like pattern has been created to simulate manually planned behaviour of the AUV. To ensure a fair comparison between the different algorithms, the number of visited grid cells have been kept consistent between the simulations.

4.6   Validation of the simulation model

To verify the different parts of the simulation model, various methods needs to be used. To validate the path planning algorithms, the first method is to establish a baseline for the simulation results. To establish this baseline, a lawn mower pattern has been created, which would be similar to a manually planned operation.

To verify the objective function based on uncertainty described in section 3.8.2, increasing uncertainty at specific locations has been performed to confirm the correct behaviour.

4.6.1   Validation through Monte Carlo simulations

To evaluate the performance of path planning using a combination of uncertainty and magnitude, the Monte Carlo method has been used to verify the performance of the algorithm. This procedure is only performed for the adaptive sampling, and does not provide additional information for the algorithm based purely on uncertainty, as this algorithm will provide the same sampling path independent of the temperature distribution.

The sampling path of the AUV with a given static field will be deterministic for all path planning algorithms used in this thesis. For the coverage-driven algorithms this path will not be influenced by the temperature field. For the data-driven algorithm, the path will be dependant on the temperature field, which makes Monte Carlo simulations applicable.

For the distribution of the sampling algorithm, the skewness and kurtosis are not needed. The goal of the simulations are not to produce a probability distribution for the sampling algorithm, but rather to present the overall performance and variance of performance. Therefore the presented data will consist of the mean and standard deviation of coverage, presented in equation (3.23) and for the different percentiles of temperature. The percentiles of 50, 70 and 90, have been used as thresholds to determine time spent within the 50, 30 and 10 percent highest temperatures. This method could be directly translated to fields of salinity and chlorophyll-A, using concentrations instead of temperature magnitude.
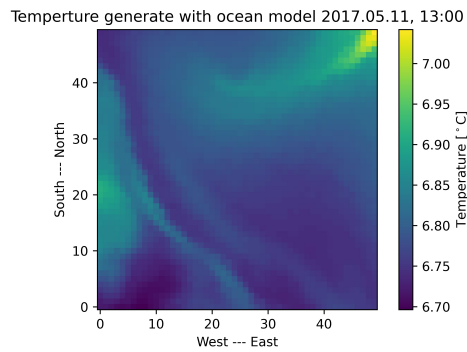
4.7   Ocean data

To further evaluate the performance of the different path planning algorithms, an ocean model created using the SINMOD ocean model has been used. This model has been created based on measured data from the 11.05.2017 to 12.05.2017 outside of Frøya in Norway.

A total of five different temperature fields from the ocean model have been used to evaluate the performance of the path planning algorithms.

Table 4.2: Overview of the different ocean samples used for evaluation of path planning algorithms. Visualisation of the fields are shown in Figure 4.3.

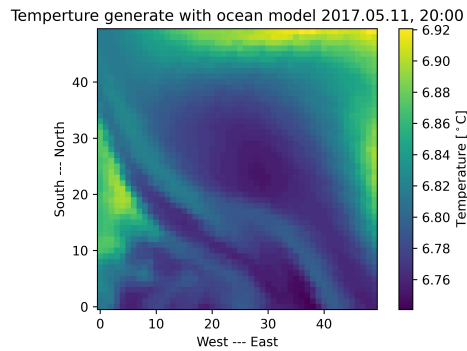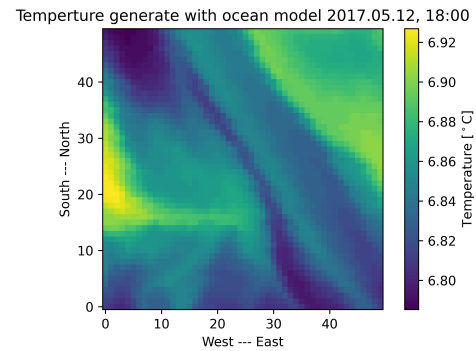| Field number	Date and time
Ocean model 1	2017.05.11, 13:00
Ocean model 2	2017.05.11, 20:00
Ocean model 3	2017.05.12, 15:00
Ocean model 4	2017.05.12, 18:00
Ocean model 5	2017.05.11, 10:00

4.7.1   Ocean models

(a) Temperature plot using measured ocean data.
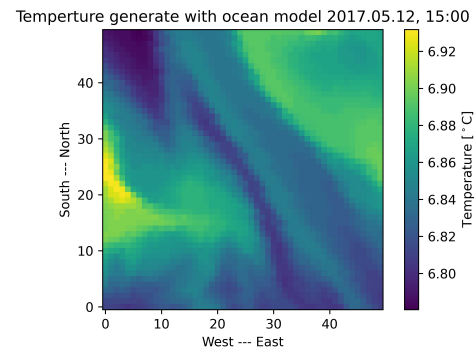
(b) Temperature plot using measured ocean data.

(c) Temperature plot using measured ocean data.

(d) Temperature plot using measured ocean data.
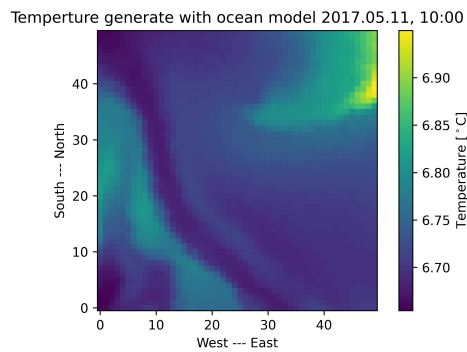
(e) Temperature plot using measured ocean data.

Figure 4.3: Temperature plots of the ocean data collected from the SINMOD ocean model, used for AUV path planning.

4.7.2   Synthetic ocean models

To show the influence of the design parameters described in subsection 4.3.1, five random fields using different design values are presented.
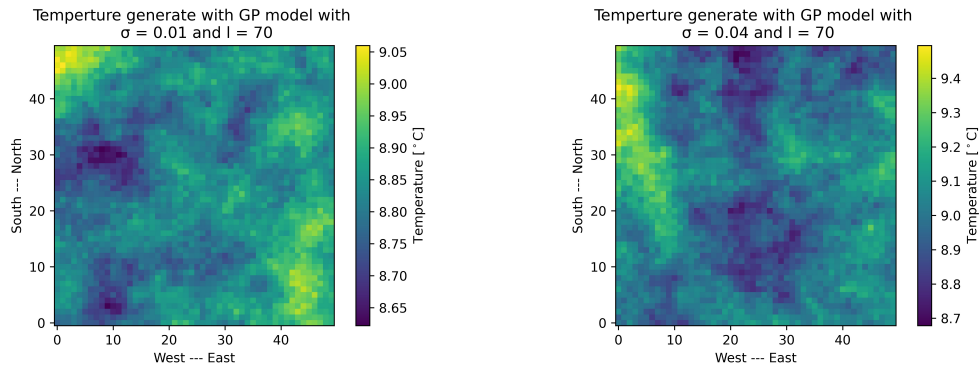
(a) Temperature field generated with $\sigma = 0.01$ and correlation length $= 70$.

(b) Temperature field generated with $\sigma = 0.04$ and correlation length $= 70$.
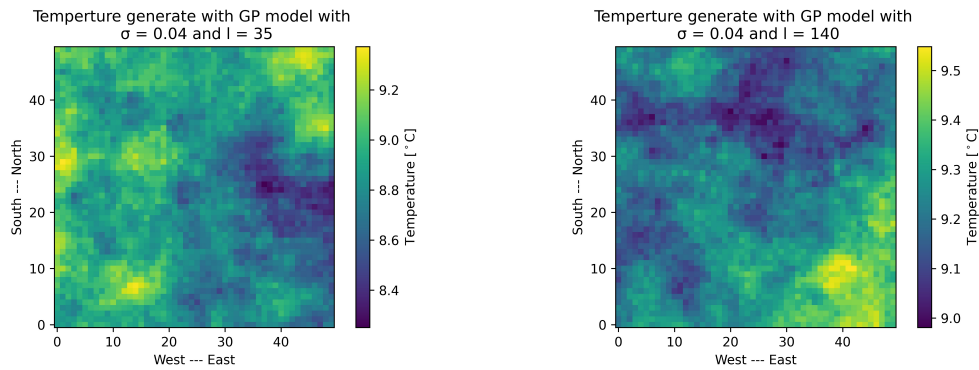
(c) Temperature field generated with $\sigma = 0.04$ and correlation length $= 35$.

(d) Temperature field generated with $\sigma = 0.04$ and correlation length $= 140$.
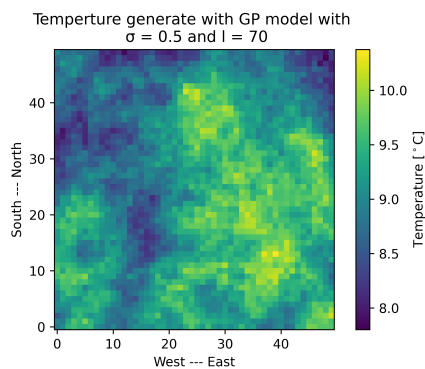
(e) Temperature field generated with $\sigma = 0.5$ and correlation length $= 70$.

Figure 4.4: Examples of temperature fields created using different hyperparameters.

Chapter 5

Results

In this chapter the results from the simulations. All simulation runs have been given the input parameters provided in chapter 4. In total four different weighting factors have been used for Monte Carlo simulations in generate random fields. For each set of weighting factors, five parameters have been recorded.

5.1 Lawn mower pattern

To establish a baseline for performance comparison a path similar to a manually planned mission is shown in this section.

5.1.1 Using a sythetic ocean model
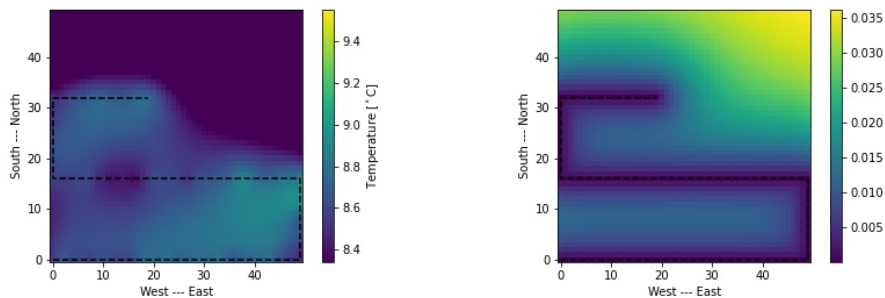
(a) Posterior temperature prediction.

(b) Posterior uncertainty prediction.

Figure 5.1: Posterior plots from a lawn mower like sampling pattern using an ocean model based on simulated data.

5.1.2 Using an ocean model based on real data

The sampled field is presented in Figure 4.3b.
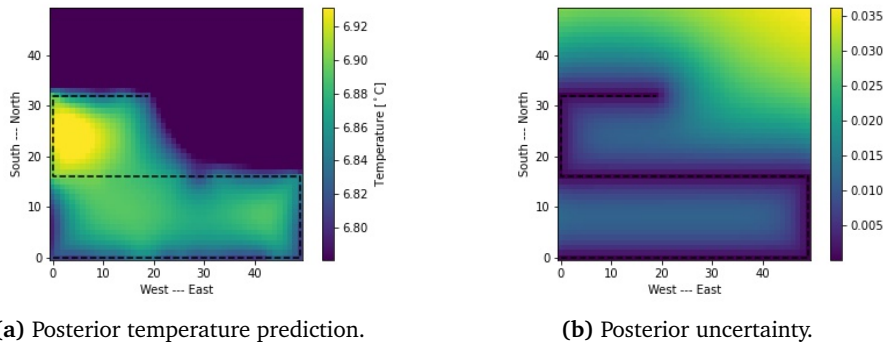
(a) Posterior temperature prediction.

(b) Posterior uncertainty.

Figure 5.2: Posterior plots from a lawn mower like sampling pattern using an ocean model based on real data.

5.2 Uncertainty algorithm

To create an uncertainty-driven algorithm, equation (3.18) has been used. Utilising the covariance matrix from the GP model, the algorithms aim to reduce the overall uncertainty of the field, by reducing the uncertainty found on the diagonal of the matrix.
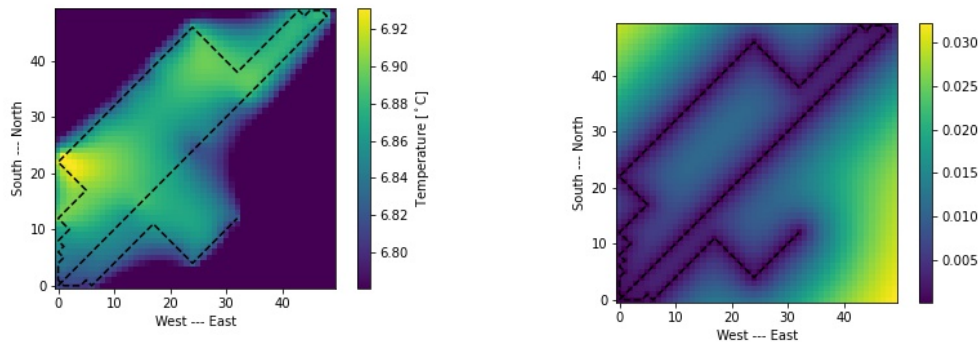
(a) Temperature prediction from the uncertainty algorithm using the SINMOD ocean model. Ocean model 2 from Table 4.2 was used

(b) Posterior uncertainty using the uncertainty algorithm.

Figure 5.3: Posterior temperature and uncertainty fields using the greedy variance algorithm for path planning.

5.3 Uncertainty with magnitude of measurement

The results using an algorithm based on equation (3.19) with the weighting parameters presented in Table 4.1, is presented in this section.

5.3.1 Simulation 1 - $\theta_1 = 0.9, \theta_2 = 0.1$

Using the data-driven algorithm presented in equation (3.19), with weighting factors $\theta = 0.9, \theta_2 = 0.1$.

Table 5.1: Results from using ocean models based on real data. Performed using $\theta_1 = 0.9$ and $\theta_2 = 0.1$.

	$\mathbf{R}^2$	RMSE	50% threshold	70% threshold	90% threshold
Ocean model 1	81.22%	0.334	60.26%	45.70%	27.15%
Ocean model 2	81.22%	0.352	60.26%	41.06%	15.89%
Ocean model 3	81.22%	0.352	58.28%	35.76%	15.23%
Ocean model 4	81.22%	0.352	60.93%	37.09%	10.60%
Ocean model 5	81.22%	0.336	51.66%	37.75%	19.87%

Table 5.2: Results from the Monte Carlo simulations performed using $\theta_1 = 0.9$ and $\theta_2 = 0.1$.

|	$\mathbf{R}^2$	RMSE	50% threshold	70% threshold	90% threshold
Number of trials	1477	1477	477	477	477
Mean	76.14%	0.459	47.45%	28.99%	10.01%
Median	73.75%	0.472	47.33%	29.33%	10.00%
Standard deviation	3.82	0.073	12.16	10.32	5.98
Maximum	81.27%	0.61	75.33%	62.00%	28.67%
Minimum	72.15%	0.28	16.00%	0.67%	0%
Mean std. error	0.099	0.002	0.558	0.470	0.274
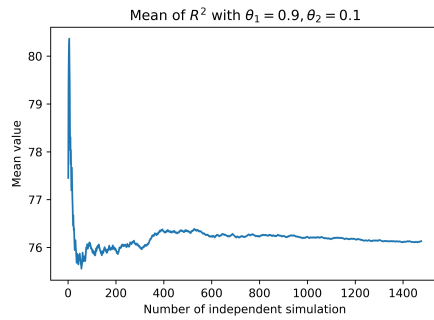
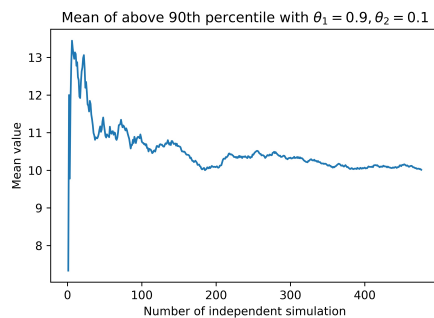**(a)** Mean of R^2 as a function of number of simulations.
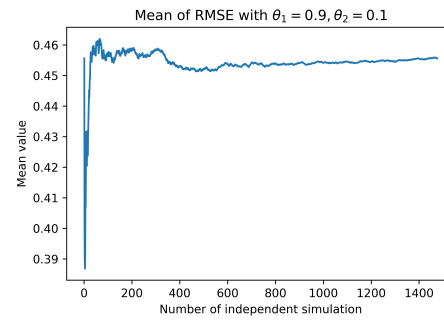
(b) Mean of RMSE as a function of number of simulations.
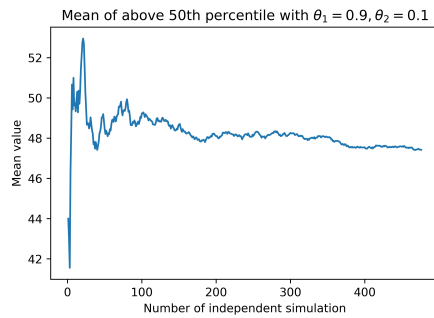
(c) Mean of time spent above the 50th percentile as a function of number of simulations.
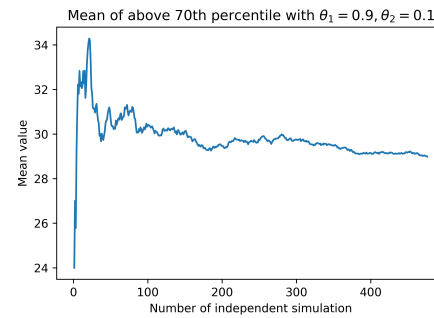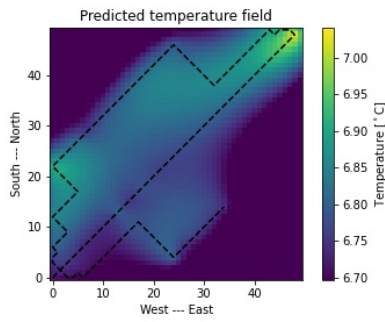

(d) Mean of time spent above the 70th percentile as a function of number of simulations.
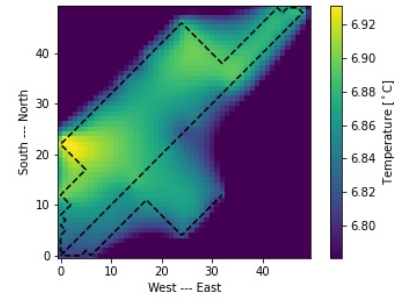

(e) Mean of time spent above the 90th percentile as a function of number of simulations.
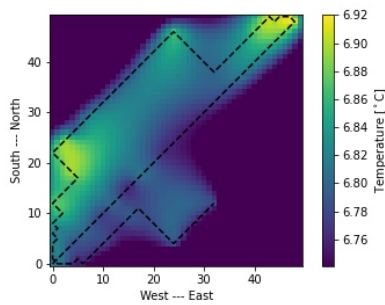
Figure 5.4: Convergence of different recorded parameters during simulations using a data-driven path planning with inclusion of magnitude. Weighted with parameters $\theta_1 = 0.9$ and $\theta_2 = 0.1$.
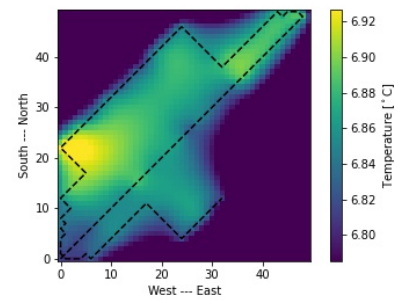
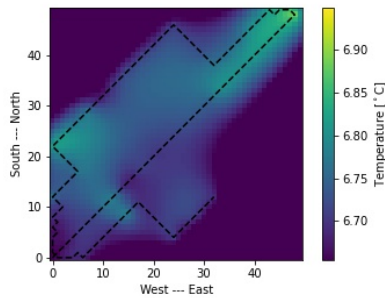**(a)** Predicted temperature field using data-driven path planning in Figure 4.3a.

(b) Predicted temperature field using data-driven path planning in Figure 4.3b.

(c) Predicted temperature field using data-driven path planning in Figure 4.3c.

(d) Predicted temperature field using data-driven path planning in Figure 4.3d.

(e) Predicted temperature field using data-driven path planning in Figure 4.3e.

Figure 5.5: Sampling path in ocean fields based on real data using $\theta_1 = 0.9$ and $\theta_2 = 0.1$.

### 5.3.2   Simulation 2 - $\theta = 0.8, \theta_2 = 0.2$

Using the data-driven algorithm presented in equation (3.19), with weighting factors $\theta = 0.8, \theta_2 = 0.2$.

Table 5.3: Results from using ocean models based on real data. Performed using $\theta_1 = 0.8$ and $\theta_2 = 0.2$.

	R^2	RMSE	50% threshold	70% threshold	90% threshold
Ocean model 1	78.12%	0.399	58.28%	45.03%	27.15%
Ocean model 2	74.33%	0.478	70.20%	46.36%	17.22%
Ocean model 3	77.94%	0.415	61.59%	36.42%	17.22%
Ocean model 4	74.33%	0.478	66.89%	41.72%	11.92%
Ocean model 5	74.28%	0.454	68.21%	45.03%	21.19%

Table 5.4: Results from the Monte Carlo simulations performed using $\theta_1 = 0.8$ and $\theta_2 = 0.2$.

|	R^2	RMSE	50% threshold	70% threshold	90% threshold
Number of trials	1614	1614	934	934	934
Mean	75.55%	0.474	48.86%	29.61%	10.06%
Median	74.28%	0.486	48.67%	30.00%	10.00%
Standard deviation	2.99	0.064	11.91	10.61	6.09
Maximum	84.91%	0.618	86.00%	56.67%	28.67%
Minimum	72.14%	0.271	15.33%	1.33%	0%
Mean std. error	0.074	0.002	0.390	0.348	0.199
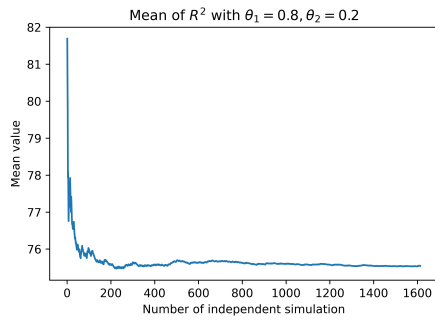
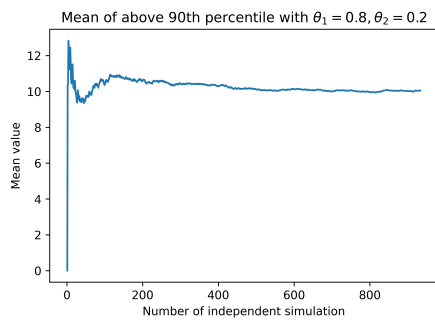**(a)** Mean of **R**^{2} as a function of number of simulations.
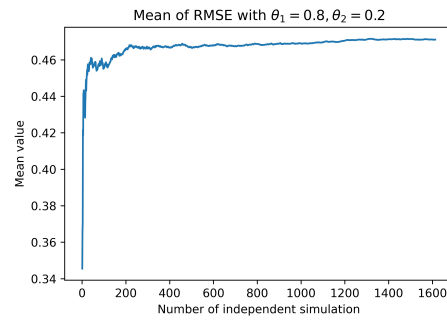
(b) Mean of RMSE as a function of number of simulations.
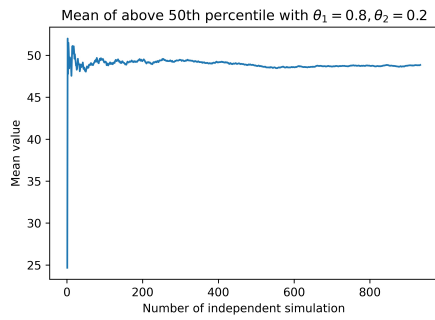
(c) Mean of time spent above the 50th percentile as a function of number of simulations.
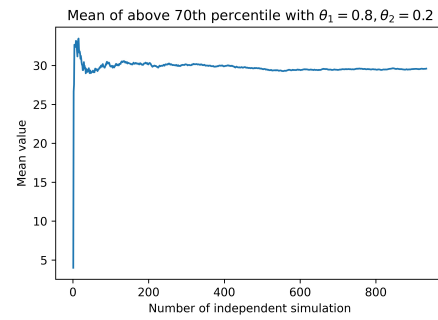
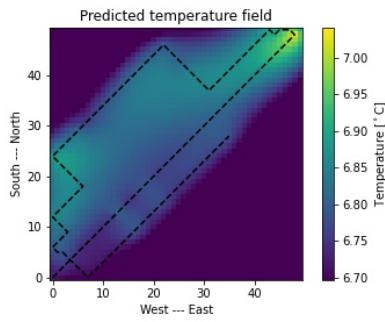
(d) Mean of time spent above the 70th percentile as a function of number of simulations.
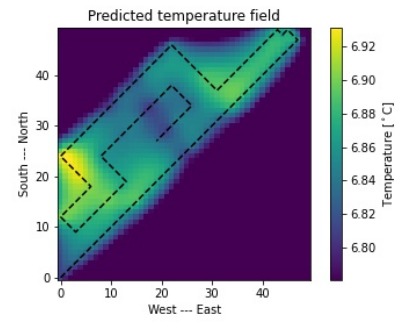

(e) Mean of time spent above the 90th percentile as a function of number of simulations.
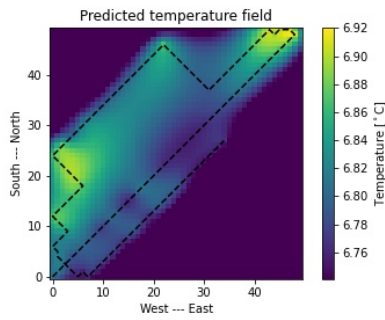
Figure 5.6: Convergence of different recorded parameters during simulations using a data-driven path planning with inclusion of magnitude. Weighted with parameters $\theta_1 = 0.8$ and $\theta_2 = 0.2$.

(a) Predicted temperature field using data-driven path planning in Figure 4.3a.

(b) Predicted temperature field using data-driven path planning in Figure 4.3b.

(c) Predicted temperature field using data-driven path planning in Figure 4.3c.
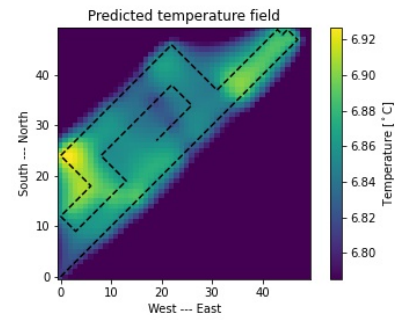
(d) Predicted temperature field using data-driven path planning in Figure 4.3d.
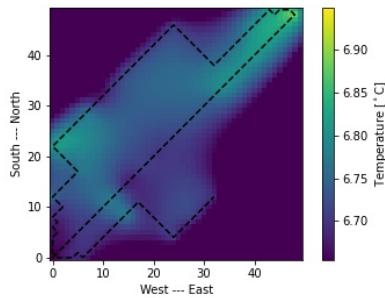
(e) Predicted temperature field using data-driven path planning in Figure 4.3e.

Figure 5.7: Sampling path in ocean fields based on real data using $\theta_1 = 0.8$ and $\theta_2 = 0.2$.

5.3.3 Simulation 3 - $\theta = 0.6, \theta_2 = 0.4$

Using the data-driven algorithm presented in equation (3.19), with weighting factors $\theta = 0.6, \theta_2 = 0.4$.

Table 5.5: Results from using ocean models based on real data. Performed using $\theta_1 = 0.6$ and $\theta_2 = 0.4$.

	$\mathbf{R}^2$	RMSE	50% threshold	70% threshold	90% threshold
Ocean model 1	85.81%	0.266	64.90%	41.06%	18.54%
Ocean model 2	86.26%	0.268	61.59%	40.40%	13.91%
Ocean model 3	78.65%	0.409	54.97%	32.45%	9.27%
Ocean model 4	86.26%	0.266	58.28%	45.03%	12.58%
Ocean model 5	80.40%	0.364	58.28%	43.05%	19.87%

Table 5.6: Results from the Monte Carlo simulations performed using $\theta_1 = 0.6$ and $\theta_2 = 0.4$.

	$\mathbf{R}^2$	RMSE	50% threshold	70% threshold	90% threshold
Number of trials	511	511	511	511	511
Mean	79.33%	0.398	48.80%	29.5%	10.02%
Median	80.43%	0.407	49.33%	29.8%	10.00%
Standard deviation	5.03	0.097	10.62	8.94	5.30
Maximum	87.09%	0.611	74.00%	50.67%	24.00%
Minimum	57.55%	0.141	19.33%	0%	0%
Mean std. error	0.223	0.004	0.470	0.399	0.235
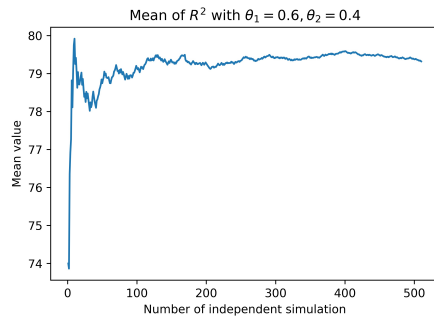
(a) Mean of R^2 as a function of number of simulations.
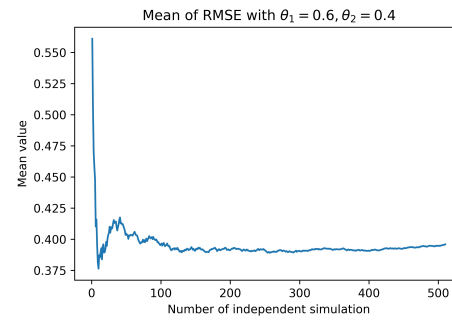
(b) Mean of RMSE as a function of simulations.
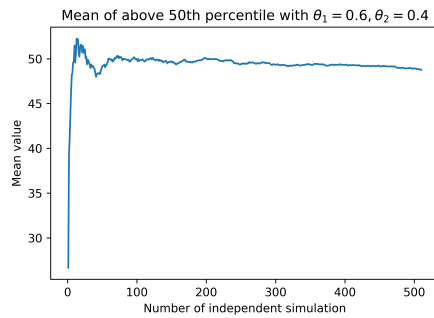
(c) Mean of time spent above the 50th percentile as a function of number of simulations.
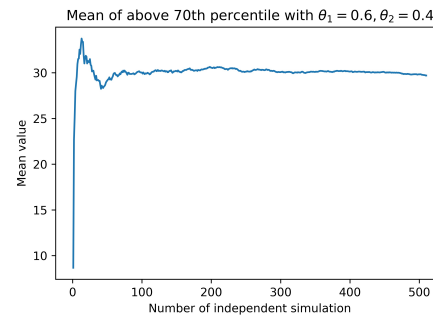
(d) Mean of time spent above the 70th percentile as a function of number of simulations.

(e) Mean of time spent above the 90th percentile as a function of number of simulations.

Figure 5.8: Convergence of different recorded parameters during simulations using a data-driven path planning with inclusion of magnitude. Weighted with parameters $\theta_1 = 0.6$ and $\theta_2 = 0.4$.
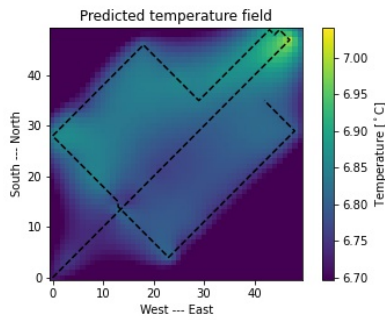
(a) Predicted temperature field using data-driven path planning in Figure 4.3a.
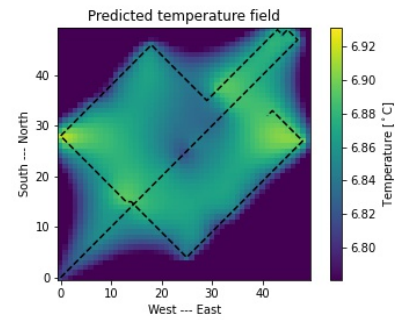
(b) Predicted temperature field using data-driven path planning in Figure 4.3b.
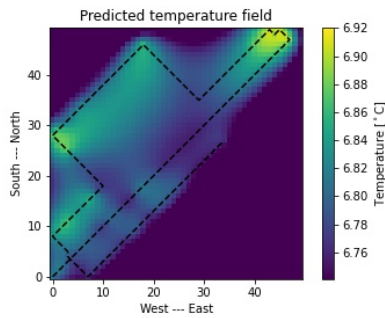
(c) Predicted temperature field using data-driven path planning in Figure 4.3c.

(d) Predicted temperature field using data-driven path planning in Figure 4.3d.

(e) Predicted temperature field using data-driven path planning in Figure 4.3e.

Figure 5.9: Sampling path in ocean fields based on real data using $\theta_1 = 0.6$ and $\theta_2 = 0.4$.

5.3.4 Simulation 4 - $\theta = 0.5, \theta_2 = 0.5$

Using the data-driven algorithm presented in equation (3.19), with weighting factors $\theta = 0.5, \theta_2 = 0.5$.

Table 5.7: Results from using ocean models based on real data. Performed using $\theta_1 = 0.5$ and $\theta_2 = 0.5$.

	R^2	RMSE	50% threshold	70% threshold	90% threshold
Ocean model 1	87.11%	0.230	45.70%	37.75%	15.89%
Ocean model 2	86.97%	0.242	63.58%	34.44%	3.97%
Ocean model 3	86.98%	0.250	54.97%	25.83%	6.62%
Ocean model 4	86.73%	0.252	51.66%	33.77%	2.65%
Ocean model 5	81.11%	0.332	68.21%	58.28%	19.21%

Table 5.8: Results from the Monte Carlo simulations performed using $\theta_1 = 0.5$ and $\theta_2 = 0.5$.

	R^2	RMSE	50% threshold	70% threshold	90% threshold
Number of trials	780	780	780	780	780
Mean	79.73%	0.381	46.84%	28.06%	9.49%
Median	81.47%	0.371	48.00%	28.67%	9.33%
Standard deviation	6.71	0.116	11.27	9.35	5.19
Maximum	87.20%	0.73	72.67%	53.33%	26.67%
Minimum	57.50%	0.135	4.00%	0.67%	0%
Mean std. error	0.240	0.004	0.404	0.335	0.186
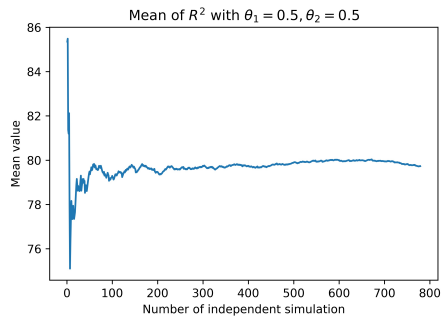
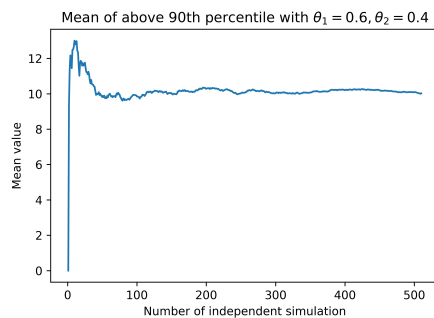**(a)** Mean of $\mathbf{R}^2$ as a function of number of simulations.
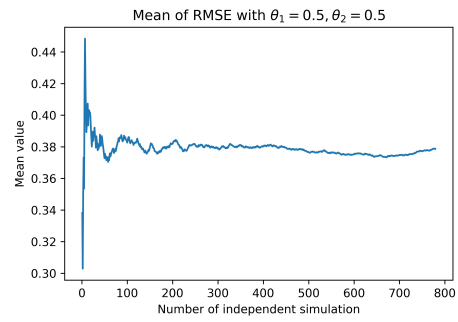
(b) Mean of RMSE as a function of number of simulations.
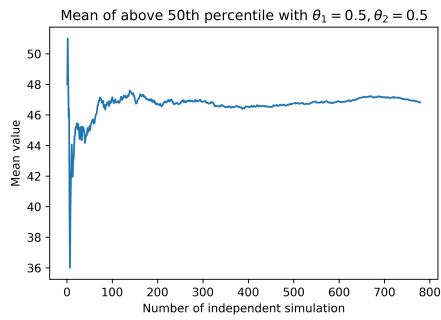
(c) Mean of time spent above the 50th percentile as a function of number of simulations.
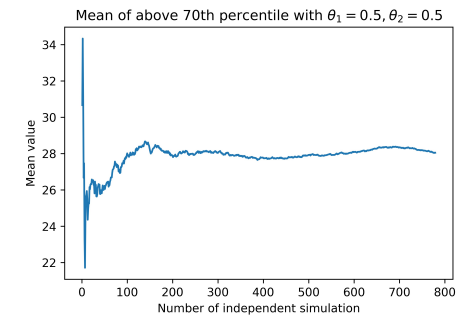

(d) Mean of time spent above the 70th percentile as a function of number of simulations.
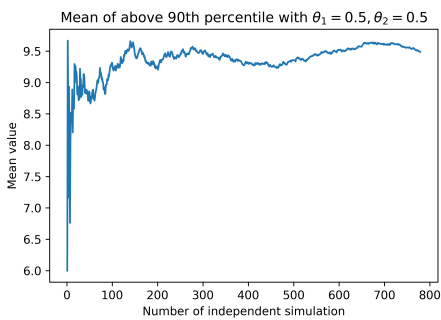

(e) Mean of time spent above the 90th percentile as a function of number of simulations.

Figure 5.10: Convergence of different recorded parameters during simulations using a data-driven path planning with inclusion of magnitude. Weighted with parameters $\theta_1 = 0.5$ and $\theta_2 = 0.5$.
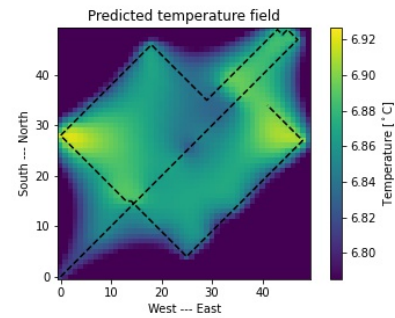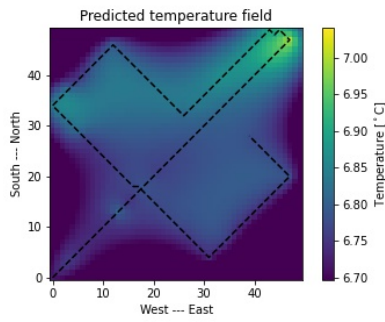
(a) Predicted temperature field using data-driven path planning in Figure 4.3a.
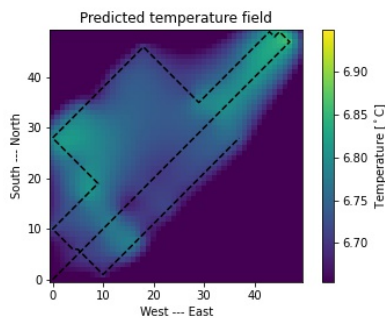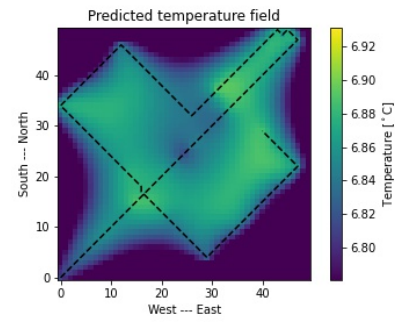

(b) Predicted temperature field using data-driven path planning in Figure 4.3b.
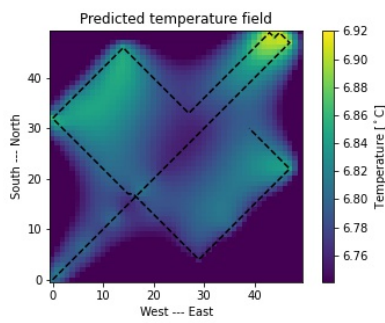
(c) Predicted temperature field using data-driven path planning in Figure 4.3c.
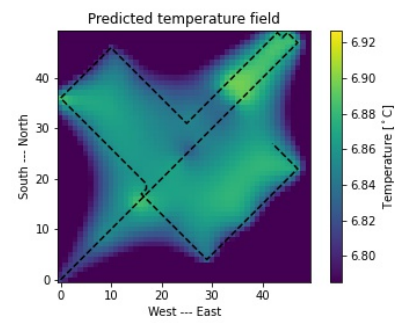
(d) Predicted temperature field using data-driven path planning in Figure 4.3d.
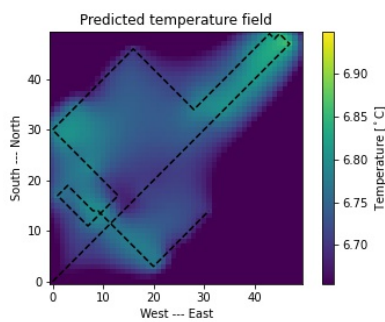
(e) Predicted temperature field using data-driven path planning in Figure 4.3e.

Figure 5.11: Sampling path in ocean fields based on real data using $\theta_1 = 0.5$ and $\theta_2 = 0.5$.

5.4 Comparison of results

To allow for better comparison of the presented data, the mean value of the different sampling strategies are presented in this section.

Table 5.9: Coverage of the different sampling strategies.

Strategy	R^2
Lawn mower	65.17%
Variance (greedy)	80.29%

Table 5.10: Comparison of mean of performance metrics for the uncertainty and lawn mower algorithms using the real ocean models.

	Lawn mower	Variance (greedy)
RMSE	0.476	0.358
50% threshold	35.07%	58.8%
70% threshold	26.67%	39.73%
90% threshold	13.73%	17.87%

Table 5.11: Comparison of mean of performance metrics from the different simulation sets, using synthetic data.

	Simulation 1	Simulation 2	Simulation 3	Simulation 4
R^2	76.14%	75.55%	79.33%	79.73%
RMSE	0.459	0.474	0.398	0.381
50% threshold	47.14%	48.54%	48.48%	46.53%
70% threshold	28.8%	29.4%	29.5%	27.88%
90% threshold	9.94%	9.99%	9.95%	9.43%

Table 5.12: Comparison of mean of performance metrics from the different simulation sets, using ocean data.

	Simulation 1	Simulation 2	Simulation 3	Simulation 4
R^2	81.22%	75.80%	83.48%	85.78%
RMSE	0.345	0.445	0.315	0.261
50% threshold	58.28%	65.03%	59.60%	56.82%
70% threshold	39.47%	42.91%	40.40%	38.01%
90% threshold	17.75%	18.94%	14.83%	9.69%

Chapter 6

Discussion

In this chapter the results presented in chapter 5 will be be discussed and evaluated according to performance criterion provided in chapter 3 and 4.

6.1 General remarks

The first simulation is weighted most heavily towards exploration, when compared to the other simulations, with the second simulation being weighted between the first and third simulation.

   The recorded parameters used as performance metrics are important to compare the performance of the different sampling strategies. The RMSE does not provide a metric to compare the posterior temperature prediction to the sampled field, as the difference between the prior temperature prediction and the temperatures found in the sampled temperature fields are too significant. This causes the RMSE to be heavily dependant on the overall coverage, which is described by $\mathbf{R}^2$.

   The $\mathbf{R}^2$ is a metric which shows the total reduced uncertainty of the field. This means the difference between the diagonal of initial covariance matrix and the posterior covariance matrix is important. $\mathbf{R}^2$ is then best increased by exploring new areas, which have not been explored. The initial path for all data-driven simulations, were along the diagonal of the field. This is due to the decrease in uncertainty of the overall field, by moving towards the centre of the field. After reaching the centre of the field the AUV moves away from the already measured areas of the field.

   Using different percentiles of temperatures as a performance metric, allows for a better understanding of the difference in collected data, between the coverage-driven and data-driven algorithms. Without a metric for "how good" the collected data is, using a pure coverage-based approach could provide better results. However, the goal of the data-driven algorithm is not to increase the overall coverage of the area, but rather to increase the utility of each measurement. Similarly to the established temperature thresholds, similar thresholds can be created for salinity and Chlorophyll-a. When measuring a biological process in the ocean, it is important to measure in locations which contain biological matter. Measurements from areas without biological matter does not provide the same insight into

the ongoing processes. It might therefore be natural to increase the influence of the measurement magnitude in these applications.

6.2   Gaussian process model

The overall goal of the GP model is to create a synthetic model of the ocean, in order to simulate performance of different path planning algorithms. The overall output from the GP which was implemented within the AUV, seems to perform according to the desired behaviour. The posterior temperature predictions provide an understanding of the visited areas of the field. The temperature prediction outside of the sampled areas tend to be colder than the temperatures found in the field in which the temperatures are found. This seems correct according to the use of an initial estimate of $5°C$ in the entire field. Altering the correlation distance influences how rapid the temperature is outside of this range, which is also as expected.

Using different hyperparameters for creation of the temperature field and GP on the AUV have not been considered. This could influence the results, as it is not realistic to be able to use these parameters directly.

A general problem related to Gaussian modelling is the increase in computational intensity, when the set of possible sampling locations grow. The grid used in this application is 50×50 grid cells, meaning the total covariance matrix has dimensions 2500×2500. Decreasing the grid spacing, thereby increasing the number of grid cells, would quickly increase the computational load significantly. To reduce this effect, different measures could be implemented. Some approaches are discussed in Bauer et al. (2017), Vanhatalo et al. (2010) and Krishnamoorthy et al. (2013).

6.3   Monte Carlo simulations

Monte Carlo simulations have been performed in order to quantify the performance of the data-driven algorithm. For the uncertainty-driven path planning algorithms, Monte Carlo simulations are not necessary as these will provide a deterministic path, independent of the stochastic field. To evaluate the different weightings of the data-driven sampling algorithm, Monte Carlo simulations need to be performed until the solution has converged sufficiently. Shown in Figure 5.4, 5.6, 5.8 and 5.10 are the convergence of different recorded parameters. In Figure 5.4a, 5.6a and 5.6b, the amount of simulations are higher than the other figures presented in Figure 5.4 and 5.6 respectively, as some of these simulations were conducted before establishing the need for temperature thresholds to quantify the performance of the path planning algorithms.

6.3.1   Usefulness of Monte Carlo simulations

The usefulness of the Monte Carlo simulations stem from the need to validate the performance of data-driven path planning in stochastic data. The different metrics provided in subsection 3.8.3, need not only to be evaluated using a single generated field, but to show the

overall performance of the different algorithms is several different fields. This provides a good foundation to use Monte Carlo simulations. Firstly, the all simulations and generations of temperature field are independent. Secondly, to be able to show the overall performance of the data-driven algorithm, it needs to be evaluated in multiple different fields to quantify the performance metrics implemented.

6.3.2   Convergence

As previously stated the convergence of different weightings of equation (3.19) are shown in Figure 5.4, 5.6, 5.8 and 5.10. The true mean of these weights could be difficult to compute exactly, which means reviewing the convergence from simulations provide a simpler and still relatively robust foundation to compare their performance.

From Figure 5.4a and 5.6a the convergence of the coverage metric R^2 is shown. As these are based on significantly more simulations when compared to the other metrics, these have been used to determine the needed number of simulations for the other weightings. Due to the simulation time of each simulation, the number of simulations for the other weightings have been reduced as the overall value of the mean does not change significantly after about 500 simulations. Even though the standard mean error is higher for the simulations where the amount of simulations has been reduced, the overall impact is not large enough when compared to the increased computational time needed.

6.4   Synthetic ocean data

The overall performance of the data-driven path planning algorithm with different weightings are shown in Table 5.2, 5.4, 5.6 and 5.8. In addition to these tables, a comparison between the mean of the different strategies is presented in Table 5.11. As previously mentioned the design parameters for the synthetic ocean model have been kept constant.

6.4.1   Algorithm performance

The overall performance of the data-driven path planning in generated temperature fields is shown in Table 5.11. For all sets of weighting parameters the overall performance is lower than expected, as the results show that the time spent above the established thresholds are lower than the remaining percentage of data.

Overall the general loss of coverage using a data-driven algorithm is expected. This is due to the algorithm no longer always choosing to move to the area which reduces the overall uncertainty the most, but could also move to an area in which the expected temperature is higher. The general trend of exploring the diagonal of the field is largely kept. There are multiple reasons for this. Firstly, the prior estimate of the temperature in the field is set to a constant $5°C$, which means the initial estimation of all nearby points is equal, making the AUV prioritise the path which reduces the uncertainty by the most. Secondly, the weighting parameters used does still largely favour *Exploration* over *Exploitation*. Thereby only changing path when the change in uncertainty reduction between two point are relatively similar,

and the temperature prediction in a certain direction is favoured.

6.4.2   Data-driven compared to coverage-driven

As previously stated, only the data-driven path planning has been conducted using Monte Carlo simulations. However, the results from these simulations can still be compared to the coverage-driven algorithm, as these types of simulations are not needed. The overall coverage of the data-driven algorithm is reduced compared to the greedy variance algorithm.

When compared to the baseline of a manually planned operation, it is clear that the overall coverage of the mission area is increased drastically. The R^2 metric of the adaptive algorithm more closely resembles that of the greedy coverage algorithm than the manually planned mission. The time spent above the established temperature thresholds should be similar between the two non-adaptive algorithms, as these take no input from the temperature field.

When compared to the greedy variance algorithm, the performance of the adaptive sampling seems to have lower coverage in general. This is expected as the adaptive algorithm, not only prioritises decreasing the overall uncertainty. As Monte Carlo simulations have not been performed for the coverage-driven algorithms, a direct comparison for the temperature thresholds is not possible. However, it is possible to assume this performance should be within the same range the results presented in Table 5.11. As the algorithm takes no input from the temperature field, moving to a grid cell within the upper 50% or lower 50% of the field should be equally likely, assuming the temperature in general is evenly distributed within the field.

6.5   Results using SINMOD ocean model

The overall paths of the AUV stayed relatively similar when using the same weighting between exploration and exploitation. The first simulation, used a identical path for all five ocean fields. This path is also very similar to the coverage-driven path planning without the inclusion of measurement magnitude. This is due to the decrease of uncertainty dominating the path planning strategy when large temperature changes are not expected from the posterior temperature prediction. In the second simulation, the AUV has chosen two different paths. The first shown in Figure 5.7a, 5.7c and 5.7e. In this path the coverage of the area is decreased, as path planning strategy favours moving along the diagonal, due to the expected temperature along this trajectory. The second path shown in Figure 5.7b and 5.7d, the expected temperature on the north side of the diagonal causes the AUV to never cross the diagonal. Using a greedy algorithm, the diagonal is highly disfavoured as the uncertainty along the diagonal is low.

The coverage of the different sampling strategies presented in Table 5.12 shows that even though simulation 1 and 2 are weighted more heavily towards exploration, they have a lower coverage R^2. The reason for this can be found when looking at the pictures presented in Figure 5.5, 5.7, 5.9 and 5.11. The coverage of simulation 3 and 4 are heavily influenced

by crossing the diagonal of the field. The influence of the data-driven criterion, causes the path to avoid the *myopic trap* of avoiding the diagonal of the field too heavily.

From the RMSE shown in Table 5.1 it is clear that the RMSE is highly dependent on the spatial coverage. In Table 5.12 the RMSE is highest for simulation 2, which has the lowest coverage. The RMSE is the lowest for simulation 4, which also has the highest coverage in the real ocean models.

Using collected field from the SINMOD ocean model does not fully account for the temporal effects of the ocean. As can be seen from Figure 4.3a compared to Figure 4.3e, during this three hour span, the relative change in temperature distribution is low. The same effect can be viewed from Figure 4.3b and 4.3d. In the case of simulation 1, the overall temperature field showed little effect on the overall path of AUV. For all simulations the AUV did not predict the higher temperature to the south, after moving along the diagonal of the field, this temperature was not captured. This causes the performance in ocean model 5 to be lower than that of ocean model 1, although this fields look similar. The difference in performance in Figure 4.3b and 4.3d is, however, not as significant as for Figure 4.3a compared to Figure 4.3e. All simulations chose similar paths in these two fields, thereby providing similar coverage in these fields. The paths chosen provided better results in Figure 4.3b than 4.3d, as reducing the uncertainty while collecting higher temperatures, better coincided with Figure 4.3b than 4.3d.

6.6   Simulated data vs real data

For the data-driven strategy, there was a clear discrepancy in performance between the synthetic and real data. There are multiple reason as to why this is the case. Firstly, the assumption in the creation of the synthetic ocean models are that the correlation length is constant, both because the field should be anisotropic from a given point, but also within the entire field it self. Due to the turbulent nature of ocean observations, this assumption could in some cases be fitting and other cases provide a significant deviation.

An important factor to consider when comparing the simulated data to real data is that the correlation length and variance of the simulated field is known, while for the real data these are unknown factors. The GP model on the AUV is used with the same hyperparameters as used to create the simulated temperature fields. This is not possible for the ocean fields created using real data. This is an important factor when comparing the results from the different simulations.

Accounting for time variability is a problem related to both modelling and planning. This is due to ocean currents, and mixing in the ocean causes a degradation of information over time. This is an important aspect which is not covered in the simulated and real data.

For data-driven applications, using the temperature gradient could be beneficial. Following gradients allow for increased resolution of ocean fronts, which could be areas of interest. Using the temperature gradient would provide quite different path, than those produced from the data-driven algorithm used in this thesis. The benefit of this can more clearly be seen from Figure 4.3 than 4.4, as there are clear ocean fronts, which could be areas of interest.

6.6.1   Algorithm performance

The performance of the uncertainty-based algorithms is not affected by whether the field is created synthetically or based on real data, as no data from this field is part of the path planning algorithm. Thus, the overall performance of the uncertainty-driven algorithm will not be affected by data from the ocean model. On the other hand the sample size of non-synthetic fields are considerably smaller than for the synthetic fields, which could influence the results significantly. The underlying parameters such as correlation length, will however affect the performance. Changing the correlation length of the GP model, will alter the chosen path of the AUV.

The performance of the data-driven algorithms was significantly increased when used in field based on ocean data. There are multiple factors which could contribute to the increase in performance. Firstly, the performance of the greedy variance algorithm is higher than expected, meaning that the increase in performance could stem from that the path chosen by this algorithm being closer to optimal in these cases. Although the performance in the ocean fields collected from the SINMOD ocean model is higher than for the synthetic ocean field, the performance is still within the range of the simulations, meaning these results could occur for a set of synthetic temperature fields.

An important factor to consider for the overall algorithm performance is the manner in which, the AUV calculates the waypoints. For the data-driven algorithm, the AUV uses the reduction of uncertainty by moving to a certain point and the predicted temperature in that point. Moving along the diagonal of the field, the AUV therefore does not capture a difference in temperature on each side of the AUV. This means the AUV is not likely to change path of the diagonal unless there is a rapid decrease in temperature along the diagonal, combined with a high enough weighting of exploitation. This does not occur for any of the simulations.

Using the lowest measured temperature in the field to normalise the influence of the measurement magnitude, causes the mean of synthetic ocean models to be important. As the overall temperature of the synthetic field are higher than those of the real fields, this impacts the significance of the measurement temp in the data-driven algorithm. The variance of the synthetically generated fields also seem to be larger than those of the real ocean models, which counteracts this effect. By normalising the magnitude term of equation (3.19) using the lowest measured temperature, the overall performance becomes more alike for fields with the same mean and variability.

Chapter 7

Conclusions

In total the overall scope of the thesis has been covered. A literature review of relevant concepts has been conducted in order to provide a theoretical background for the conducted work. The implementation of the simulations has been conducted in Python, due to the limitations in using the open-source software provided in the LSTS toolchain. A GP model of ocean temperature has been created and implemented, based on a model provided by Trygve O. Fossum, to create synthetic temperature fields which resembles an ocean model. An adaptive sampling algorithm has been developed and tested, together with an algorithm using only uncertainty for path planning and a path planning strategy, close to a "lawn mower" pattern. This was to better compared the performance to a manually planned mission. To better evaluate the performance of the algorithm, different performance metrics have been considered and implemented. Lastly, the adaptive algorithm has been used in both synthetic ocean temperature fields and using the SINMOD ocean model. To compare these results, Monte Carlo simulations have been conducted to provide a better understanding of the algorithms performance in synthetic ocean temperature fields.

Going back to the research questions formulated in section 1.3, these can be discussed based on the results provided in chapter 5. Using different weighting between uncertainty and measurement magnitude, provided in Table 4.1, the standard deviation from the Monte Carlo simulations generally is reduced for higher influences of the measurement magnitude.

7.1 Algorithm performance

The overall performance of the algorithms utilising the covariance matrix of the GP model, was significantly better than the manually planned path. The difference in performance between the synthetic ocean model and the models from the SINMOD ocean model, was significant, but within the expected maximum and minimum of the Monte Carlo simulations. Using a higher weighting towards the temperature magnitude, caused the overall coverage in the ocean models to be increased, as these simulations avoided the myopic trap of avoiding the initial transect of the field.

The from the established performance metric, the adaptive sampling algorithm did not provide significant increase or decrease in performance in the synthetic ocean fields. There

could be different reasons for this, which are discussed in chapter 6. In the real ocean fields, all sets of weighting factors performed significantly above simulations in synthetic temperature fields.

Using the RMSE as a performance metric, proved to be redundant, as it was too dependant on the overall coverage of the mission area. $\mathbf{R}^2$ provided a good metric for the coverage of the operation, while the temperature percentiles are needed in order to examine the algorithms utility. Using other performance metrics might have proven to be beneficial.

7.2   Recommendations for further work

For further work, the implemented simulation model could expanded to include multiple different features. Implementing different path planning algorithms could be part of future work related to this thesis. These path planning algorithms could aim for a non-myopic approach, where the planning horizon is increased compared to the greedy algorithms used in this thesis. This does however impose the need to handle non-modelled time-variability.

Using the SINMOD ocean model more actively, by including the temporal effects of simulations using this model should also be considered. Although the temperature fields collected from the SINMOD model, seem to be similar, the temporal effects of the ocean are not fully considered without the use of this type of model.

The GP model used during this thesis has assumed an isotropic process, which for further would should be evaluated to include the anisotropic properties of the ocean. Online reevaluation of the hyperparameters in the GP has also not be considered, but could be part of future work.

Using multiple different vehicles at once is also a natural step towards a more synoptic coverage of the area. This could increase both coverage and sampling density, while improving performance off all vehicles due to a common knowledge base.

References

[1] M Bauer et al. 'Understanding Probabilistic Sparse Gaussian Process Approximations'. In: (2017), p. 9.

[2] Jonathan Binney et al. 'Informative Path Planning for an Autonomous Underwater Vehicle'. In: (2010), p. 6.

[3] Nannan Cao et al. 'Multi-Robot Informative Path Planning for Active Sensing of Environmental Phenomena: A Tale of Two Algorithms'. In: (2013), p. 15.

[4] Thomas B. Curtin et al. 'Autnomous Oceanographic Sampling Networks'. In: (1993).

[5] Trygve O. Fossum. 'Adaptive Sampling for Marine Robotics'. In: (2019).

[6] S Frolov. 'Enabling Technologies for Data Assimilation in a Coastal-Margin Observatory'. 2007.

[7] Paul Glasserman. *Monte Carlo Methods in Financial Engineering*. Springer, 2003.

[8] Levent Koçkesen et al. *An introduction to Game Theory*. 2007.

[9] Aravindh Krishnamoorthy et al. 'Matrix Inversion using Cholesky Decomposition'. In: (2013), p. 3.

[10] Dirk P. Kroese and Zdravko I. Botev. 'Spatial Process Generation'. In: (2013).

[11] Dirk P. Kroese, Tim Brereton et al. 'Why the Monte Carlo method is so important today'. In: (2014). DOI: https://doi.org/10.1002/wics.1314.

[12] Erik G. Learned-Miller. 'Entropy and Mutual Information'. In: (2013).

[13] N. E. Leonard et al. 'Collective Motion, Sensor Networks, and Ocean Sampling'. In: (2007).

[14] Pierre F.J. Lermusiaux et al. 'Quantifying Uncertainties in Ocean Predictions'. In: (2015). DOI: https://doi.org/10.5670/oceanog.2006.93.

[15] Kian H. Low et al. 'Adaptive Multi-Robot Wide-Area Exploration and Mapping'. In: (2008).

[16] Jonatan Olofsson et al. 'Multi-agent informed path planning using the probability hypothesis density'. In: (2020).

[17] *Percentile rank*. May 2021. URL: https://en.wikipedia.org/wiki/Percentile_rank.

[18] José Pinto et al. 'Multiple Autonomous Vehicles Applied to Plume Detection and Tracking'. In: (2018). DOI: 10.1109/OCEANSKOBE.2018.8558802.

[19] Samik Raychaudhuri. 'Introduction to Monte Carlo simulation'. In: (2008), p. 10. DOI: 10.1109/WSC.2008.4736059.

[20] S. Riser et al. 'Fifteen years of ocean observations with the global Argo array'. In: (2016). DOI: https://doi.org/10.1038/nclimate2872.

[21] Dean Roemmich et al. 'Autonomous Profiling Floats: Workhorse for Broad-scale Ocean Observations'. In: (2004). DOI: https://doi.org/10.4031/002533204787522802.

[22] Stuart Russel et al. *Artificial Intelligence, A Modern Approach*. Pearson Education Limited, 2016.

[23] O. Schofield et al. 'The Robot Ocean Network'. In: (2013).

[24] Mae L. Seto. *Marine Robot Autonomy*. Springer, 2013.

[25] Sintef. *SINMOD*. URL: https://www.sintef.no/sinmod/#/.

[26] J Vanhatalo et al. 'Approximate inference for disease mapping with sparse Gaussian process'. In: (2010), p. 28. DOI: 10.1002/sim.3895.

Appendix A

Appendix

Code and other files used throughout the master thesis is provided at:
https://gitlab.com/aurlab/student/simulation/-/tree/MartinSkaugset-master-patch-13263
Alternatively the code without the ocean model can be found at:
https://github.com/MartinSkaugset/Master